Earth Sciences
2023; 12(5): 121-139
http://www.sciencepublishinggroup.com/j/earth
doi: 10.11648/j.earth.20231205.12
ISSN: 2328-5974 (Print); ISSN: 2328-5982 (Online)

On the Timing and Nature of Magmatism in the North Atlantic Igneous Province: New Implications from Basaltic Rocks of the Faroe Islands

Jógvan Hansen[1], Morgan Ganerød[2]

[1]HansenReSearch, Torshavn, Faroe Islands

[2]Geological Survey of Norway, Trondheim, Norway

Email address:
jogvanha@hotmail.com (Jógvan Hansen), jogvan.hansen@dunelm.org.uk (Jógvan Hansen), morgan.ganerod@ngu.no (Morgan Ganerød)

To cite this article:
Jógvan Hansen, Morgan Ganerød. On the Timing and Nature of Magmatism in the North Atlantic Igneous Province: New Implications from Basaltic Rocks of the Faroe Islands. *Earth Sciences*. Vol. 12, No. 5, 2023, pp. 121-139. doi: 10.11648/j.earth.20231205.12

Received: August 2, 2023; **Accepted**: September 1, 2023; **Published**: September 27, 2023

Abstract: In this contribution we present novel radiometric $^{40}Ar/^{39}Ar$ ages representing a number of basaltic sills/lavas of the Faroe Islands, which themselves form part of the North Atlantic Igneous Province. Measured ages are utilised in an attempt to assess the local igneous history, where the new ages are contrasted against those of other local rocks of known ages as well as against those of comparable/neighbouring North Atlantic igneous regions. The novel ages presented in this contribution allow us to put new constraints on the timing of late stage magmatic activity and associated crustal extension of this part of the North Atlantic area. In this research we present new ages as young as ~50.5 Ma for some of the smallest Faroese sills and demonstrate that the larger and oldest local sills, grouped into the low-TiO_2 Streymoy/Kvívík sills and the high-TiO_2 Eysturoy/Sundini sills respectively (~55.5 Ma), likely formed immediately subsequent to the formation of the uppermost parts of the Enni Formation, which itself represent the latest stages of local surface magmatism at ~55.8 Ma. Gradually decreasing sill volumes coupled with successively younger ages point to systematic decrease of local igneous activity with increasing distances to active contemporaneous local rifting zones. Comparable scenarios recorded for other parts of the North Atlantic Igneous Province support our inferences regarding the nature of late-stage magmatic activity at some distances from zones of active seafloor-spreading. Comparisons between ages of Faroese igneous products versus those of e. g. central E Greenland point to a somewhat diachronous evolution pattern within this part of the North Atlantic Igneous Province subsequent to ~57.5 Ma. The lithosphere-asthenosphere boundary is commonly thought to be critical for the formation of basaltic magmas. Accordingly, the close spatial and temporal associations between many high-TiO_2 and low-TiO_2 Faroese rock suites are interpreted in the context of a regional version of this boundary.

Keywords: Timing Nature Magmatism, North Atlantic Igneous Province, Faroe Islands, Flood Basalts, Sill Intrusions, $^{40}Ar/^{39}Ar$ Geochronology, Petrogenetic Interpretations

1. Introduction

Basaltic rocks of the Faroe Islands Basalt Group (FIBG) form part of the North Atlantic Igneous Province (NAIP), which itself is one of the Large Igneous Provinces (LIPs) on Planet Earth [1, 2]. Combined, the igneous regions of the NAIP encompass vast areas in the North Atlantic such as in the eastern parts of the Baffin Island, in West Greenland, in East Greenland, offshore West Norway (Vøring and Møre basins), in the Faroe Islands, on the Rockall Plateau and in the NW British Isles [3] (Figure 1A). Igneous NAIP products post-dating the main rifting event at ~55.8 Ma are to be found in Iceland and adjacent submerged Greenland-Iceland and Iceland-Faroes ridges, in Jan Mayen (smaller scale), in West and East Greenland, in submerged igneous seamounts in the Norwegian-Greenland Sea, on either side of the Reykjanes ridge, at the eastern fringes of the Rockall Plateau and in the Rockall Trough [3-6]

Magmatic events within the various igneous regions of the NAIP have traditionally been associated with incipient crustal extension in the Early Paleogene Period along axes in the Labrador Sea, offshore East Greenland and in the Rockall

Trough through the Shetland Basin respectively, followed by active extension-related seafloor-spreading in the NE Atlantic and in the Labrador Sea [1, 4, 7, 8]. Hence, reliable radiometric age determinations of representative igneous products within the various parts of the NAIP are essential to determine the magmatic development along the various extension/rift axes so as to evaluate the timing of lithospheric stretching that occurred in the various igneous regions prior to, contemporaneous to and subsequent to initiation of active seafloor spreading.

In this contribution we present for the first time $^{40}Ar/^{39}Ar$ ages for a number of basaltic sills intruded into the lava succession of the Faroe Islands and for a one key local lava flow. A few $^{40}Ar/^{39}Ar$ ages on local lava flows from previous research [9, 3] are presented in conjunction with results of this research. Obtained new radiometric ages from the actual research are in turn utilised in order to assess/interpret the igneous evolution within the actual region in addition to being briefly contrasted against some radiometric ages of other relevant parts of the NAIP. From a more global perspective, we aim to increase the understanding of the developments of LIPs, especially during waning igneous phases within these. In this contribution we also endeavour to explain the common occurrences of close spatial and temporal co-existence of high-TiO_2 and low-TiO_2 Faroese basaltic sills and lavas in the context of mantle melting at the lithosphere-asthenosphere boundary (LAB).

2. Regional Geology

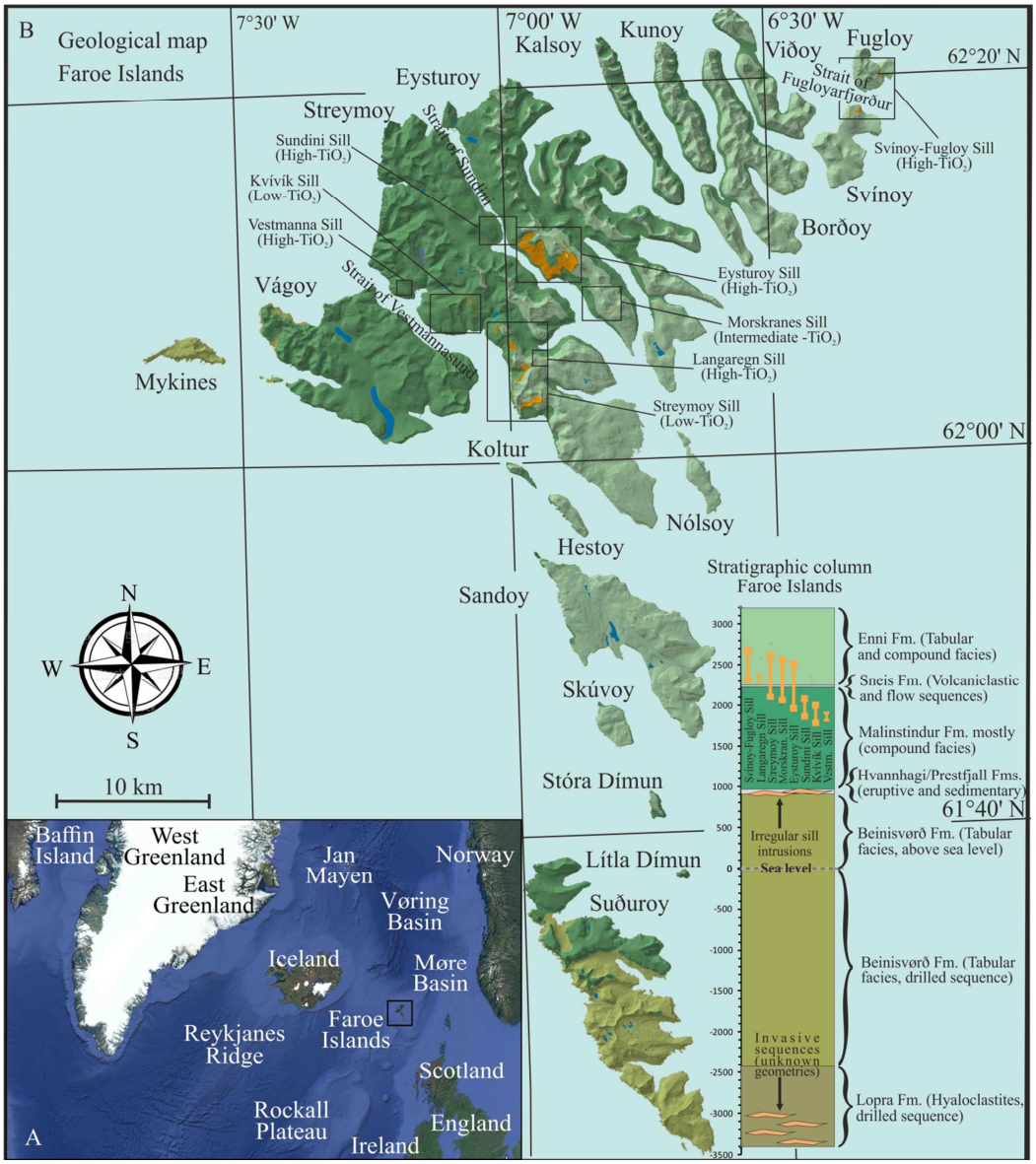

Figure 1. *Maps showing the area relevant for this study. (A) The "Google Earth" based map illustrates locations of the main parts of the NAIP, including the focus of this study the Faroe Islands. (B) The map, based on topographic data from Munin Fo, Faroe Islands, shows the main basaltic formations building up the Faroe Islands: Modified from [5, 10-12]. The stratigraphic column illustrates the thicknesses of the various geological formations according to nomenclature of Passey and Jolley [13]. Orange bars indicate total vertical (stratigraphic) extent of the actual sills. Simplistic explanation on general sill trends and extents are shown on central left of (B).*

Situated between East Greenland and the NW European continental margin, the FIBG makes up a relatively central part of the NAIP (Figure 1A). The exposed onshore parts of the Faroese basaltic lava pile cover around 1400 km^2 with a total stratigraphic extent (exposed and drilled) of around 6.6 km: [11] and refs. therein. The Faroese lava pile can be grouped into seven formations from bottom and up: the ~1075 m thick Lopra Formation; the ~3250 m thick Beinisvørð Formation; the ~9 m thick Prestfjall Formation; the 40-50 m thick Hvannhagi Formation; the 1250-1350 m thick Malinstindur Formation; the up to ~30 m thick Sneis Formation and finally the ~900 m thick Enni Formation, which might have been a few hundreds of metres thicker than 900 m initially [13] (Figure 1B). The Malinstindur, Sneis and Enni formations are intruded by a few basaltic transgressive (saucer-shaped) sills of various extent and thicknesses, which likely represent the latest manifestations of igneous activity within the actual region [10, 11, 14]. Hence, the actual sills postdate all known extrusive activity in the actual area, but their absolute/radiometric ages have not been known prior to this research.

A few attempts to estimate/measure age (s) of Faroese lavas have been undertaken previously, including paleomagnetic dating [15-17] and radiometric $^{40}Ar/^{39}Ar$ dating [9, 18]. Amongst these, the most recent ages by Storey *et al*. [9] appear to be most reliable and consistent with ages of comparable basaltic lavas from other parts of the NAIP. Their age determinations pointed to ages of ~60 Ma for the bottom of the Beinisvørð Formation and ~57 Ma for its top sections, while they measured an age of ~55.2 Ma for upper sections of the Enni Formation.

3. Materials and Methods

3.1. Sampling and Petrography

Initially, samples were collected from 7 Faroese sills (the Streymoy, Kvívík, Eysturoy, Morskranes, Svínoy-Fugloy, Langaregn and Vestmanna sills) and a key Faroese lava flow, i. e. the bottom of the Malinstindur Formation, as shown in Electronic Supplement B. [19]. Noticeable proportions of the exposed parts of the Faroese sills are intensely jointed and/or have been exposed to chemical weathering. As the main bodies of individual Faroese sills display quite homogeneous petrography and geochemistry [5, 11], the foremost sampling criterion involved the acquirement of fresh specimen. Hence, great care was taken to collect representative sill and lava samples without joints or visible signs of weathering at the whole-rock scale. Due to the homogeneous nature of the actual sills, most of the sill samples represented the bulk of their main bodies displaying medium-grained texture (Streymoy, Kvívík, Eysturoy, Svínoy-Fugloy and Morskranes sills), while samples of the much smaller Langaregn Sill in addition to the lava sample from the bottom of the Malinstindur Formation exhibited relatively fine-grained textures [19], in accordance with characteristics typical of their main/bulk bodies. The fine to medium grained and homogeneous Vestmanna Sill [e.g. 19] probably experienced a crystallising history between these two categories. Physical dimensions, general petrography and geochemistry for the bulk of Faroese sills and lavas have also been detailed in previous studies [5, 10, 11, 20].

Most of the actual $^{40}Ar/^{39}Ar$ analyses are based upon groundmass material, whilst plagioclase was used for a couple of samples (Table 1, Figure 2). Reasonable/acceptable reproducibility in repeated $^{40}Ar/^{39}Ar$ analyses of groundmass and/or plagioclase crystals determined which analyses were accepted for presentation in this contribution. As it turned out, only a couple of plagioclase analyses generated results acceptable for this paper, while groundmass analyses yielded the best results for the rest of the samples. Sample qualities at the whole-rock scale were assessed on thin-sections (microscopy) and on major elements, determined by means of X-ray fluorescence (XRF) analyses, as shown in Electronic Supplement B [19].

3.2. Analytical Techniques

Samples were crushed and sieved to obtain 180 – 250 μm fractions. The finer particles were decanted in tap water and the coarser residue further ultrasonically washed in acetone and de-ionized water several times. The grains deemed by optical investigations to be best suited, being void of any coatings, were handpicked under a stereomicroscope. The samples were packed in aluminium capsules together with the Taylor Creek Rhyolite (TCR) flux monitor standard along with zero age reagent grade K_2SO_4 and optical grade CaF_2 salts for interference corrections. The samples were irradiated at the MTA reactor (Hungary) for c. 2 hours, with a nominal fast neutron flux density of c. 5.5×10^{13} $n*(cm^{-2} *s^{-1})$. The interference correction factors for the production of isotopes from Ca and K are shown in Table 1. Groundmass and plagioclase materials were placed in a 3.5mm pit size aluminium sample disk and step heated using a defocused 3.5 mm CO_2 laser beam from Photon Machine Fusions 10.6 with a flat energy spectrum. The extracted gases from the sample cell were expanded into a Piston Free Stirling Cryocooler for trapping potential water vapour and further into a two-stage low volume extraction line (c. 300 cm^3), both stages equipped with SAES GP-50 (st101 alloy) getters, the first running hot (c. 350°C) and the second running at room temperature. The samples were analyzed with a MAP 215–50 mass spectrometer in static mode, installed at the Geological Survey of Norway. The peaks and baseline (AMU = 36.2) were determined during peak hopping for 15 cycles (15 integrations per cycle, 30 integrations on mass ^{36}Ar) on the different masses ($^{40–36}Ar$) on a MasCom electron multiplier (MC217) in analogue mode and linearly regressed back to zero inlet time. Blanks were analyzed every third measurement. After blank correction, a correction for mass fractionation, ^{37}Ar and ^{39}Ar decay and neutron-induced interference reactions produced in the reactor was undertaken using in-house software AgeMonster, written by M. Ganerød. It implements the equations from [21] and the recently proposed decay constant for ^{40}K after [22]. A $^{40}Ar/^{36}Ar$ ratio of 298.56±0.31 from [23], was used for the atmospheric

argon correction and mass discrimination calculation using a power law distribution of the masses. We calculated J-values (irradiation flux parameter) relative to an age of 28.619±0.036 Ma for the TCR fluence monitor [22]. We used the following criteria to determine the sample ages: at least 3 overlapping consecutive steps (95% confidence), accounting of more than 50% cumulative ^{39}Ar released from the spectra analyses.

4. Results

When it comes to the basaltic sills of the Faroe Islands, it was known on beforehand that they must be younger than the local Enni Formation at ~55.8 Ma, which most of them intrude. The ± uncertainties in measured ages for some of the dated material (Table 1), do in a few instances result in overlapping ages for analysed samples, which in theory could weaken some of the arguments presented below. Associated diagrams, involving Cumulative % 39Ar released versus K/Ca and % Radiogenic 40Ar ratio plots in addition to isochron (39Ar(k)/40Ar(a+r) versus 36Ar(a)/40Ar(a+r) ratios) diagrams, are illustrated in Electronic Supplement A, [24], Figure A and Figure B.

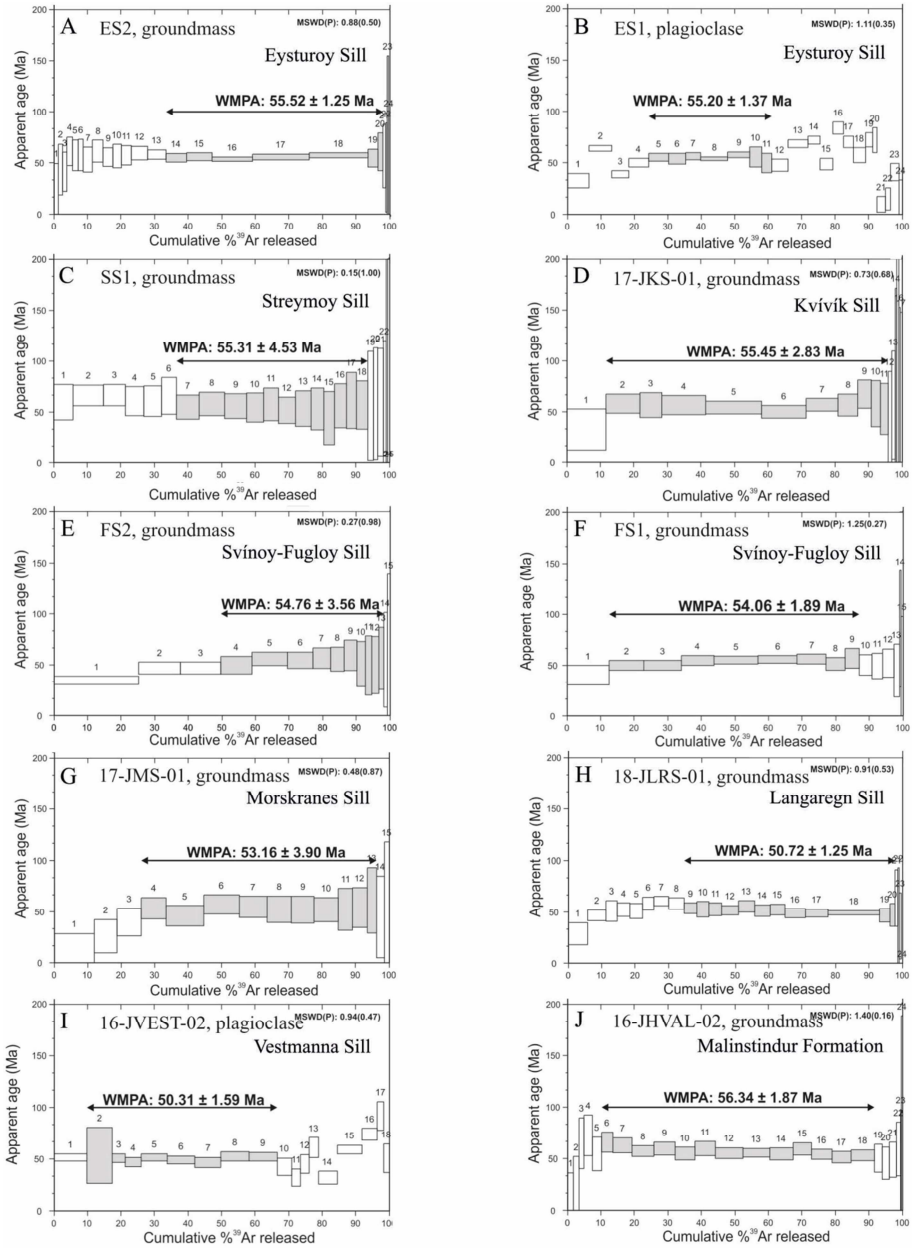

Figure 2. *Age spectra for seven basaltic sills and one selected local lava flow of the Faroe Islands from Table 1. Individual plateau ages (± 1.96σ), presented according to interpretations of individual steps versus cumulative % ^{39}Ar release, are indicated on individual part figures. Individual incremental-heating steps (boxes), used for age determinations are indicated in grey colour. Associated K/Ca and % radiogenic ^{40}Ar versus cumulative % ^{39}Ar release diagrams are presented in electronic Supplement A [24]. (A) and (B) represent two samples of the High-TiO$_2$ Eysturoy Sill; (C) and (D) represent two samples of the low-TiO$_2$ Streymoy and Kvívík sills respectively; (E) and (F) represent two samples from the high-TiO$_2$ Svínoy-Fugloy Sill; (G) represents the intermediate-TiO$_2$ Morskranes Sill while (H) and (I) represent the high-TiO$_2$ Langaregn and Vestmanna sills. (J) represents bottom lava flows of the Malinstindur Formation.*

Table 1. *Early Cenozoic $^{40}Ar/^{39}Ar$ ages representing sills and lavas of the Faroe Islands.*

Lavas and sills	Sample	Material	Steps (n)	Spectra			K/Ca±1.96s	Inverse isocron		
				%^{39}Ar	Age±1.96s Ma	MSWD (P)		Age±1.96s	MSWD (P)	Trapped $^{40}Ar/^{36}Ar$
Streymoy Sill	SS1	Groundmass	7-18 (12)	57.09	55.31±4.53	0.15 (1.00)	0.06426±0.00179	54.00±8.18	0.15 (1.00)	304.75±33.30
Kvívík Sill	17-JKS-01	Groundmass	2-11 (10)	84.22	55.45±2.83	0.73 (0.68)	0.04452±0.00170	56.27±6.29	0.82 (0.59)	297.47±7.92
Eysturoy Sill	ES-1	Plagioclase	5-11 (7)	36.89	55.20±1.37	1.11 (0.35)	0.07±0.00	54.36±3.91	1.29 (0.27)	309.89±48.72
Eysturoy Sill	ES-2	Groundmass	14-20 (7)	64.52	55.52±1.25	0.88 (0.50)	0.05970±0.00241	55.31±11.77	1.06 (0.38)	299.62±59.73
Svínoy-Fugloy Sill	FS-1	Groundmass	2-9 (8)	74.54	54.06±1.89	1.25 (0.27)	0.08418±0.00271	59.40±6.33	1.06 (0.39)	275.21±28.32
Svínoy-Fugloy Sill	FS-2	Groundmass	4-13 (10)	48.63	54.76±3.56	0.27 (0.98)	0.03±0.00	52.75±14.93	0.29 (0.97)	306.51±62.50
Morskranes Sill	17-JMS-01	Groundmass	4-13 (10)	70.34	53.16±3.90	0.35 (0.96)	0.02±0.00	56.77±11.48	0.35 (0.95)	291.14±23.60
Langaregn Sill	18-JLRS-01	Groundmass	9-20 (12)	63.18	50.72±1.25	0.91 (0.53)	0.02909±0.00096	39.79±9.13	0.39 (0.95)	342.72±39.38
Vestmanna Sill	16-JVEST-02	Plagioclase	2-9 (8)	56.79	50.31±1.59	0.94 (0.47)	0.00372±0.00003	58.69±8.02	0.49 (0.82)	286.12±12.12
Malinstindur FM	16-JHVAL-02	Groundmass	6-18 (13)	81.51	56.34±1.87	1.40 (0.16)	0.07827±0.00349	50.95±3.72	0.57 (0.85)	318.20±12.47

Ages are reported relative to Sanidine standard TRC (28.619 ± 0.036 Ma [22]. n = number of heating steps used/total. Age, weighted by the inverse of variance. MSWD, mean square of weighted deviations. ± 1.96s refer to the statistical 95% confidence interval.

The range in 40Ar/39Ar ages determined for the sills of this study span from ~50.3 Ma to ~55.5 Ma, i. e. a total time interval of ~5.2 million years (myr), while the age of the single local lava flow is ~56.34 Ma (Table 1; Figure 2).

Combined, the Faroese sills formed at relatively irregular intervals (Figure 2). The Streymoy, Kvívík and Eysturoy sills, which amongst themselves belong to two distinct geochemical groups (the low-TiO_2 Streymoy/Kvívík sills and the high-TiO_2 Eysturoy/Sundini sills respectively), formed at 55.2 to 55.5 Ma (average ~55.35 Ma); the High-TiO_2 Svínoy-Fugloy Sill developed at 54.1 to 54.8 Ma; the intermediate-TiO_2 Morkranes sill came into being at ~53.2 Ma while the high-TiO_2 Langaregn and Vestmanna sills formed at 50.3 to 50.7 Ma.

Clear and systematic variations exist between sill sizes/volumes relative to their measured ages. The oldest local sills (~55.35 Ma on average) display the largest volumes whereas the slightly younger Svínoy-Fugloy Sill (at ~54.45 Ma on average) is noticeably less bulky; the Morskranes Sill (at ~53.2 Ma) in turn is smaller than the Svínoy-Fugloy Sill, while the Langaregn and Vestmanna sills (at ~50.5 Ma on average) are considerably less voluminous than all other local sills [5, 10].

5. Discussion

5.1. Basic Remarks

Measured and recalculated ages representing Faroese lava formations fall well within age ranges measured for similar lava successions of other igneous regions of the NAIP such as W Greenland, E Greenland NW British Isles and sills of the Vøring Basin, offshore Norway [3, 4, 25-29, 31]. Ages recorded previously for lavas of the Faroese Malinstindur and age of the Enni formation measured in this contribution (Figure 4) straddle the proposed/estimated timeline of incipient 'main' opening phase of the North Atlantic at ~56 Ma to 55.6 Ma [3] and likely formed in association with this momentous event. Interestingly, a number of relatively recent research and reviews on evolutionary tendencies of continental margins of the NAIP, have indicated somewhat diachronous and complex evolution patterns prior to and subsequent to the initiation of the proposed 'main' rifting event at around 55.6 Ma to 56 Ma [4, 28-33].

When it comes to the driving processes necessary to initiate and maintain tectonic activity associated with momentous events such as the opening of e. g. the N Atlantic and Labrador Sea – Baffin Bay areas during the Early Paleogene Period, some authors have invoked a "bottom-up" mechanism associated with a gigantic ascending mantle plume or perhaps a couple of plumes [26, 29, 34], while others have argued in favour of a "top-down" mechanism associated with 'continental-drift' and far-field extensional stresses [30, 35, 36]. In either case, extension and thinning of the crust/lithosphere must be invoked in order to explain decompression melting and magma transport in sub-vertical dyke systems in the proto Faroe Islands area and other NAIP regions prior to, simultaneously and subsequent to the main rifting event. Earlier studies on the FIBG have consistently pointed to the formation of the Malinstindur and Enni formations subsequent to a largely quiescent/hiatus period following deposition of the thick Beinisvørð Formation, during which only limited local volcanic activity took place: [13] and refs. therein).

5.2. Ages, Geochemistry and Spatial Distribution of Faroese Sills

The entire Faroese archipelago, currently exposed above sea level, only encompass an area of ~1400 km_2 out of the supposed original ~120000 km_2 lava plateau [13]. Hence, tens or even hundreds of sills could in theory have been emplaced over a geographically wide area at various stages and periods of time during formation of the initial Faroese

basaltic plateau, of which there exist no traces at the present time. Indeed, sill complexes have been reported for other parts of the NW European border too, including offshore Norway, the Rockall trough and Faroe-Shetland Basin. Altogether, the exposed parts of the Faroese sills extend for ~50 km in an ENE-WSW direction and ~20 km in a NNW-SSE direction. Low-TiO_2 and intermediate-TiO_2 sills extend farthest to the SSE, as compared to the bulk of the high-TiO_2 sills (Figure 1B). Hence, the high-TiO_2 varieties were probably closer to the initial axis of NE-Atlantic seafloor-spreading during their formation.

Most Farose sills display slight mutual geochemical variations, but sill samples of the low-TiO_2 Streymoy-Kvívík sills and the high-TiO_2 Eysturoy-Sundini sills respectively, display identical mutual geochemistry/petrography and close spatial relationships [5, 11] (Figure 1B; Figure 3). The Streymoy and Eysturoy sills are by far the most voluminous of the Faroese sills and even more so, when combined with the Kvívík and Sundini sills respectively.

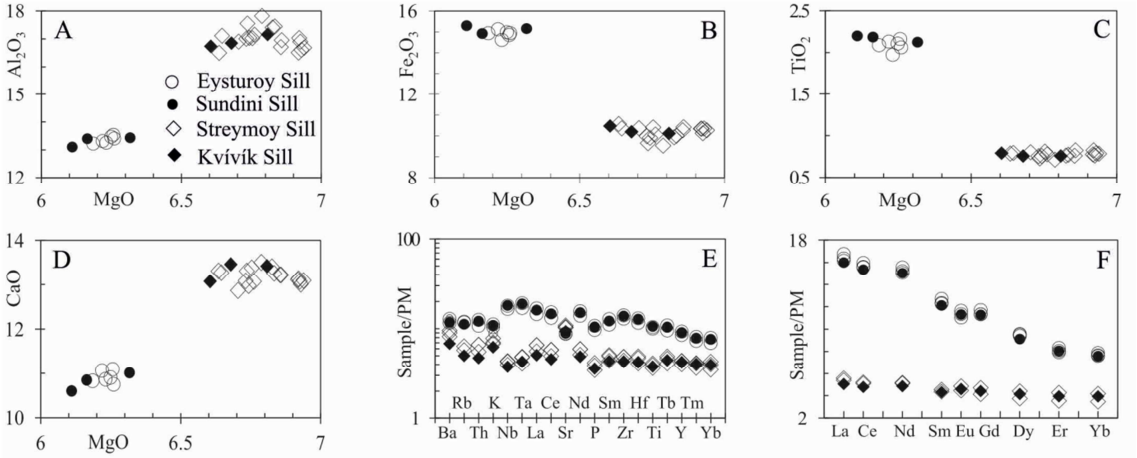

Figure 3. *The diagrams (A – F) illustrate the close geochemical similarities between the Streymoy and Kvívík sills and between the Eysturoy and Sundini sills respectively (Data from: [5, 11]. Trace elements and REE are normalised to primitive mantle (PM) values of McDonough and Sun [37].*

Hence, it is hardly surprising that the Streymoy and Kvívík sills display roughly similar $^{40}Ar/^{39}Ar$ ages with an average of ~55.35 Ma (Table 1; Figure 2C; Figure 2D). Similarly, it is overwhelmingly likely that the high-TiO_2 Eysturoy Sill, which likewise display average $^{40}Ar/^{39}Ar$ ages of ~55.35 Ma, formed contemporaneously to the Sundini Sill, considering their intimate geochemical and spatial relationship (Figure 3B).

It is well established amongst petrologists that high-TiO_2 basaltic magmas form at relatively small-degree melting of mantle material, while their low-TiO_2 counterparts develop from larger degrees of mantle melting. With respect to the large contemporaneous Faroese high-TiO_2 Eysturoy and Sundini sills, in addition to the low-TiO_2 Streymoy and Kvívík sills (average age ~55.35 Ma), it is worth noting that the average distance between these two contrasting sill groups is only ~13 km and the shortest distance a mere ~6 km (Figure 1B). Previous research have suggested that depths of the LAB define general mantle depths, at which high-TiO_2 melts presumably form at relatively great depths/pressures relative to those of their low-TiO_2 counterparts [36]. LAP depths are generally considered to increase gradually away from active rift axes. Accordingly, Faroese high-TiO_2 groups should be expected to have formed at somewhat greater mantle depths relative to their local low-TiO_2 counterparts, provided that the local LAB displayed typical seafloor-spreading architecture. If the actual low-TiO_2 sill group indeed formed at typical LAB configurations/depths, their magmas would have travelled for somewhat longer lateral distances compared to most of their contemporaneous high-TiO_2 counterparts, which were intruded closer to the then rifting zone farther to the NW. Alternatively, melting within geographically restricted and moderately heterogeneous asthenospheric and/or lithospheric mantle sources, which were variously affected by previous metasomatic/igneous events, generated the Faroese high-TiO_2 and low-TiO_2 sill groups [5, 11].

Sill ages versus volumes collectively point to a decrease in local melt production during formation of successively younger Faroese sill intrusions (Svínoy-Fugloy Sill at ~54.45 Ma; Morskranes Sill at ~53.2 Ma; Langaregn and Vestmanna sills at ~50.5 Ma).

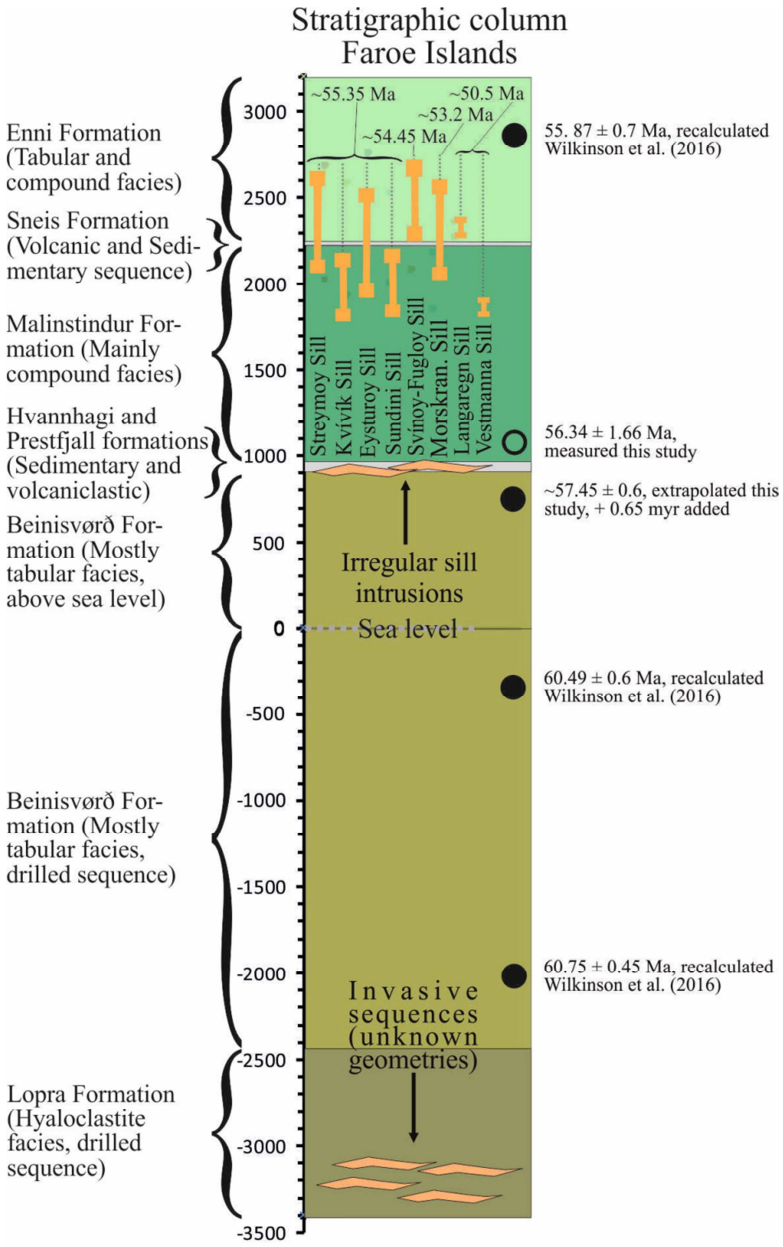

Figure 4. *$^{40}Ar/^{39}Ar$ radiometric ages of Faroese sills and selected lava formations/sequences are shown in relation to a stratigraphic column representing the basaltic rocks of the Faroe Islands (modified from Figure 1). Measured sill ages (average values) and age of the local Malinstindur Formation are from this study as presented in TABLE 1 and Figure 2. Original ages on Faroese lava formations from Storey et al. [9] and using ^{40}K decay constant from Renne et al. [38], as shown in brackets to the right of the stratigraphic column, have been replaced by recalculated ages from the compilation of Wilkinson et al. [3] with correction according to Kuiper et al. [39] and using ^{40}K decay constant of Min et al. [40]. Age for top sections of the Beinisvørð Formation is extrapolated (~0.65 myr added) based on other recalculated data for the actual region by Wilkinson et al. [3].*

5.3. Geochronology of Faroese Sills Compared to to Local Host Lavas

In the actual study we utilise a decay constant for ^{40}K after Renne *et al*. [22]. Ages obtained in this study have been contrasted with relatively recent geochronological data on other parts of the local lava pile (originally from Storey *et al*. [9], which employed ^{40}K decay constant of Renne *et al*. [38], but where we make use of recalculated ages by Wilkinson *et al*. [3] instead. Recalculated ages in the compilation of Wilkinson *et al*. [3] tend to be around 0.65 myr older than the original ones [9]. Hence, the extrapolated value shown for the top of the Beinisvørð Formation in Figure 4 result from the addition of ~0.65 myr to the original value of [9]. The radiometric $^{40}Ar/^{39}Ar$ age of ~56.34 Ma obtained in this study for the lowermost parts of the Malinstindur Formation would appear to be a realistic one, especially when compared to the recalculated ages for the top of the Beinisvørð Formation at ~57.4 Ma and for the upper parts of the Enni Formation at ~55.8 Ma respectively (Figure 4). If these ages are indeed reliable, i. e. if their measured uncertainties of 1.66 and 0.6 myr respectively are considered to be mostly theoretical, they would indicate a hiatus period, during which the sedimentary and partly volcaniclastic Hvannhagi and Prestfjall formations

were deposited, which could have lasted for up to ~1.1 myr. The entire nature of magmatism in the FIBG region appear to have changed radically from the presumed cessation of surface magmaticm at ~55.8 Ma to the onset of sill emplacement at ~55.5 Ma, which could have been triggered by e. g. reorientations or changes of magnitudes of regional principal stress axes (i. e. previous sub-sections). The Faroese region could potentially have experienced another shorter hiatus period of ~0.3 myr, lasting from cessation of local extrusive activity at ~55.8 Ma until the onset of local intrusive activity at ~55.5 Ma at the earliest. However, overlapping ages from theoretical uncertainties in measured ages renders it somewhat daring to argue in favour of a hiatus period of exactly ~0.3 myr. Also, the minimum thickness of the Enni Formation, which has commonly been estimated at >900 m (~55.8 Ma, Compilation of [3], could in theory have been several hundred metres thicker than that initially: [13] and refs. therein.

While the current preserved rims of Faroese sills are supposed to indicate their original maximum stratigraphic heights fairly accurate (top of orange bars in Figure 4), the exposed and eroded bottom sections of some of these same sills could initially have extended to somewhat lower stratigraphic levels than is indicated with the orange bars on the same figure. It is not very likely that timing of sill emplacements did significantly govern the crustal depths where these ultimately came to rest, as there are no clear correlation between measured sill ages and their relative positions with respect to geography and stratigraphy. There exist however, noticeable degrees of overlap between some of the Faroese sills with respect to their positions/levels in the local stratigraphy (Figure 1B; Figure 4).

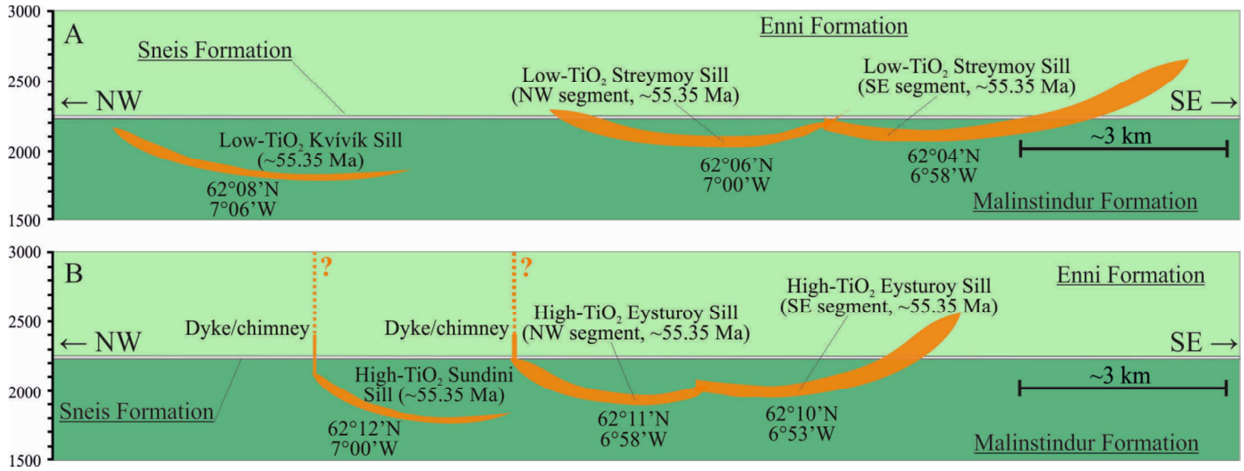

Figure 5. *The basic drawings illustrate the systematic changes in intrusion depths within two Faroese sill systems (also illustrated in Figure 1 and Figure 4), where individual sills and sill segments within each group are of identical ages. Numbers on Y axes refer to the stratigraphic columns shown in Figure 1 and in Figure 4. Views are orthogonal to longest sill axes, as these typically appear as elliptical bodies in map view. Average latitudes and longitudes for central sill sections are indicated below each intrusion. (A) Longest and shortest axes of these low-TiO_2 elliptical sills measure: Streymoy Sill, SE segment, ~5.5 x ~3.5 km; Streymoy Sill, NW segment, ~4.5 x ~2.5 km; Kvívík Sill ~4.5 x ~2.5 km. The sill segments of the Streymoy Sill are connected/welded at their NW and SE extremes respectively, while the shortest (preserved) distance to the Kvívík Sill from the NW segment of the Streymoy Sill is around 2 km in a NW direction. (B) Longest and shortest axes of the high-TiO_2 elliptical sills measure: Eysturoy Sill, SE segment, ~4 x ~3 km; Eysturoy Sill, NW segment, ~3 x ~3 km; Sundini Sill ~3 x ~3 km. Segments of the Eysturoy Sill are welded at their NW and SE extremes respectively, while the SE parts of the Sundini Sill reaches the NW extreme of the Eysturoy Sill at a relatively lower altitude. Two small sub-vertical dykes/chimneys emanate from their highest N and NW points respectively.*

Individual intrusions defining the two contemporaneous Faroese high-TiO_2 and low-TiO_2 sill groups, were initially emplaced at different stratigraphic levels, where intrusion depths increased towards the NW (Figure 4, Figure 5A, Figure 5B). Likewise, if the ~50.5 Ma Langaregn and the Vestmanna Sills are considered to represent a distinct magmatic event, they too display a general increase in intrusion depths towards the NW (Figure 4). It is noticeable that volumes for all these individual sills and segments decrease systematically from the SE towards the NW. None of the sills presented in Figure 5 display any clear differences with respect to their geographical/lateral extent. The sills and segments shown in Figure 5 also become successively thinner and less developed from the SE towards the NW. For instance, the SE segment of the Streymoy Sill is 35 – 45 m thick; the NW segment of the same sill is 10 – 30 m thick with the thinnest parts occurring at its preserved basal section towards the WSW, while the Kvívík Sill thickens from 0.5 – 1 m at its basal WSW sections to 8 – 10 m at its NE rims. These trends are more or less repeated in the Eysturoy and Sundini sills where the SE segment of the former is 45 – 55 m thick, its NW segment is 10 – 20 m thick and thinning towards its basal WSW sections, while the Sundini Sill is ~0.5 – 1 m thick at its WSW basal sections and reach a maximum thickness of 6 – 8 m at its NE rims.

The observed systematic increase in intrusion/stratigraphic levels and decrease in sill sizes/volumes towards the NW for segments of the Streymoy and Eysturoy sills and the associated Kvívík and Sundini sills respectively (Figure 5), could in theory have arisen in response to one or more of the following scenarios: 1) Their overburden [s] (i. e. the Enni Formation) systematically decreased in thickness towards the NW at the time of their emplacement, thus resulting in the sills being initiated at successively greater stratigraphic

depths towards the NW relative to e. g. the thin Sneis Formation; 2) Intrusion of sills at increasingly deeper crustal levels towards the NW prevented the sills from being fully developed/inflated due to impediment from an ever increasing overburden load; 3) Volumes of available magmas, which gave rise to these two sill systems, decreased noticeably from the SE towards the NW thus resulting in intrusions becoming sequentially less developed towards the NW due to magma starvation; 4) Successively decreasing sill sizes/volumes, coupled with a general decrease in their states of development towards the NW, could in theory result from their initial magmas being channelled directly through the thicker uppermost parts of these still immature intrusions, thus feeding local surface magmatism. However, the very restricted lateral extents of preserved dykes/chimneys on top of the Eysturoy and Sundini sills (for instance) do not suggest abundant magma transport via these intrusions (Fig.5B).

5.4. Pre- to Syn-Rift Faroe Islands Versus Neighbouring NAIP Regions

As remarked in previous sub-sections, the bulk of the igneous products associated with the evolution of the NAIP were emplaced during the Early-Middle Paleogene Period. NAIP rocks, emplaced in W Greenland at ~64 Ma to ~28 Ma, were situated ≥1250 km from the then embryonic FIBG in the Early Paleogene Period and had a somewhat complex evolution pattern associated with local extension/rift trajectories [29], while the bulk of the British Tertiary Igneous Province (emplaced at ~64 Ma to ~42 Ma) developed along an extension/rifting trajectory situated a noticeable distance to the south and southeast of the then FIBG area: e. g. [3] and refs. therein. Hence, these two NAIP regions may not be ideally suited for direct comparison with the contemporaneous FIBG area. However, NAIP regions such as central E Greenland in particular and perhaps also to some degree the N Faroe-Shetland Basin – Møre Marginal High area, all of which occur at latitudes roughly matching those of the FIBG area, appear to be better suited for comparisons with the FIBG when it comes to tectonic and magmatic evolution shortly prior to the onset of the local hiatus period at ~57.5 Ma. Moreover, coastal areas of central E Greenland, hosting the bulk of the NAIP products of that region, display basement thicknesses akin to those determined for the Faroe Islands previously [41, 42].

A recent study on offshore basaltic lavas of the N Faroe-Shetland Basin – Møre Marginal High area (including Lagavulin), which presumably were emplaced shortly prior to and perhaps contemporaneous to the inferred main N Atlantic rifting event, tentatively pointed to an origin from multiple local eruption sites and local sources in response to a localised rifting event [43]. These authors argued in favour of initial high-TiO_2 magma formation at relatively great mantle depths within the local area, as opposed to generation of their low-TiO_2 counterparts in response to melting at shallower mantle levels, the latter of which were presumably relatively more affected by regional extension/rifting.

It is noticeable that whilst the Faroese area apparently experienced a mostly relatively quiescent/hiatus period with only limited volcanism at ~57.45 Ma to ~56.35 Ma (Uncertainties considered to be mostly theoretical), noticeable quantities of broadly contemporaneous igneous products were deposited in the Blosseville Kyst area, central E Greenland in the same period of time. Incidentally, parts of the uppermost Faroese lava formations and parts of exposed E Greenland lavas have been correlated earlier based mainly on chemostratigraphic similarities [16, 44, 45]. In accordance with available $^{40}Ar/^{39}Ar$ ages, pertinent examples include: Milne Land Fm ~56.8 Ma; Nansen Fjord Fm ~58.4 Ma to ~57.5 Ma (i. e. 58.36 Ma MSWD); Sorgenfri Gletcher diabase/sill ~57.1 Ma; Tobias Dal, Upper Plateau Lava Series ~56.5 Ma: compilation of Wilkinson *et al*. [3] and refs. therein. Consequently, if we accept that there existed a general hiatus period within the Faroese area at ~57.45 Ma to 56.35 Ma (i. e. ± uncertainties are mostly theoretical), it is possible that overall stress regimes within these two neighbouring NAIP regions were somewhat dissimilar during that period of time. Here, 'some' extensional activity probably prevailed in parts of the central E Greenland area as opposed to a relatively quiet period without noticeable extensional activity in the contemporaneous FIBG area. Hence, these two regions could have been decoupled from one another tectonically during this period of time, or in any case were differently affected by contemporaneous tectonic activity.

Earlier studies have pointed to a possible compositional (chemostratigraphy) association between mostly high-TiO_2 basaltic volcanic sequences of central E Greenland (Rømer Fjord Fm and Skrænterne Fm) and the Faroe Islands (Enni Fm), all of which were presumably emplaced shortly prior to the onset of the NE Atlantic rifting [44,45]. Relatively recent high-precision zircon U-Pb geochronological data on the Skaergaard Intrusion of central E Greenland and on the associated Basistoppen Sill point to emplacement ages from ~56 Ma to ~55.85 Ma [46], while gabbros belonging to the oldest part of the neighbouring Kærven Intrusive Complex (gabbro) have yielded $^{40}Ar/^{39}Ar$ ages of around 55.8 Ma: compilation of Wilkinson *et al*. [3] and refs. therein. Hence, intrusive activity apparently took place in central E Greenland during the same period of time in which the upper lava sections of the Faroese Enni Formation were emplaced and around 0.3-0.5 myr prior to the onset of intrusive activity in earnest within the Faroese area at ~55.5 Ma (Emplacement of the oldest sills; Figure 4).

Interestingly, $^{40}Ar/^{39}Ar$ radiometric ages on central E Greenland (Blosseville Kyst) lavas of the Rømer Fjord Fm and the Skrænterne Fm, which are exposed at higher stratigraphic levels relative to the Skaergaard Intrusion, have yielded ages of ~55.84 Ma (MSWD) and ~55.69 Ma (MSWD) respectively [3]. Accordingly, both surface and intrusive magmatism within some parts of central E Greenland (notably the Kangerlussuaq Fjord area) took place during the same relatively short time span, in which lavas of the relatively young Faroese Enni and Malinstindur formations were emplaced. If dykes/chimneys emanating from tops of the NW parts of the younger Eysturoy

Sill and from the Sundini Sill (Figure 5B) indeed fed contemporaneous local surface magmatism, it must have been on a negligible/moderate scale, considering their restricted lateral extents.

Alternative causes for the recorded mismatch in igneous activity for central E Greenland versus the FIBG respectively at ~56 Ma to ~55.6 Ma (Merely extrusive activity in the Faroese area, as opposed to both intrusive and extrusive activity in the contemporaneous E Greenland area) could perhaps include: 1) The $^{40}Ar/^{39}Ar$ radiometric dating method used in the geochronological studies listed above could be less accurate than the zircon U-Pb dating system in general due to inaccurate ^{40}K decay constants for instance [47]. 2) As the oldest Early Paleogene intrusions of central E Greenland were emplaced partly in top layers of the local basement and partly in the bottom layers of local lava formations, contemporaneous hitherto undetected Faroese intrusive equivalents could in theory reside in none-exposed parts of e. g. the Lopra or Beinisvørð formations. 3) As the current extent of exposed/preserved onshore FIBG lavas represent only minor parts of the initial local lava plateau, intrusions with ages roughly similar to those of the older ones of central E Greenland could in theory have existed initially within parts of the FIBG, which were later removed by erosion (its NE fringes for instance). However, if the actual recorded/measured data and observations for these two igneous regions do indeed correctly represent igneous events in these two regions at ~56 Ma to ~55.6 Ma, it would appear that the central E Greenland area was affected by short-lived and perhaps repeated fluctuations in sizes and orientations of local principal stress axes shortly prior to the main NE Atlantic rifting event. Steady and uniform extensional forces could have prevailed within the FIBG until ~55.6 Ma, as indicated by extrusive activities. Hence, the E Greenland and Faroese regions could have been partly or wholly decoupled tectonically from one another during the time span leading up to the proposed main rifting event at ~56 Ma to ~55.6 Ma. Causative events with the potential to explain the recorded magmatic/tectonic differences between these two contemporaneous NAIP regions, could have involved the onset of northwards drifting of Greenland relative to the N American and NW European plate margins, which occurred roughly contemporaneously [48].

5.5. Post-Rift Faroe Islands Versus Neighbouring Central E Greenland

It is clear from the text and data above that while presumed pre-rift to syn-rift igneous activity within the FIBG generally occurred as extrusive magmatism (~61 Ma to ~55.8 Ma), recorded local post-rift igneous activity chiefly occurred as intrusive magmatism (~55.5 Ma to ~50.5 Ma). Post-rift igneous activity in the then neighbouring central E Greenland region was of a more diverse nature, comprising both extrusive and intrusive magmatism [3]. Post-rift volcanic successions emplaced at ~49 Ma to ~44 Ma have been recorded for Kap Dalton, central E Greenland (Blosseville Kyst), along with numerous other lava successions emplaced at ~55.5 Ma to ~53.4 Ma farther to the north along the NE Greenland coastb [3]. Formation of the Kap Dalton lavas was probably triggered by a regional rifting event [49]. Post-rift intrusive activity in central E Greenland include the Kærven Intrusive Complex (alkali granite) emplaced at 53.5 Ma to 53.3 Ma (U-Pb ages of other intrusions in the Kialineq District suggest emplacement at 37.9 Ma to 36.9 Ma [50]); intrusions of the Agtertia Fjord lineament and islands intruded at 50.3 Ma to 47.9 Ma; intrusions of the Kangerlussuaq Fjord lineament emplaced at 51.5 Ma to 46.3 Ma and intrusions of the Wiedeman Fjord – Kronborg Gletcher lineament intruded at 52.5 Ma to 37.3 Ma (These are $^{40}Ar/^{39}Ar$ ages, extrapolated from Table 1 in Tegner *et al*. [25] by the addition of around 0.7 myr to their tabulated values, which would be in accordance with age recalculations in the compilation of Wilkinson *et al*. [3]). Hence, the bulk of the post-rift intrusive activity in central E Greenland took place at intervals in the period from ~53.5 Ma to ~37 Ma. Post-breakup intrusive activity in the central E Greenland area have been attributed to re-configuration of NE Atlantic spreading ridges due to failed continental rift systems in the Kangerlussuaq Fjord region [25].

Extrusive activity along the E Greenland margin in a time span from ~55.2 to ~55.5 Ma, i. e. broadly contemporaneous to intrusions of the five oldest and largest Faroese basaltic sills, has only been recorded for lavas of NE Greenland [3]. With respect to the contemporaneous central E Greenland region, the lack of any igneous products displaying radiometric ages of ~55.6 Ma to ~53.5 Ma seem to suggest that this particular area could have experienced a relatively quiescent period during this period of time, i. e. prior to the formation of the oldest parts of Kærven Intrusive Complex [50]. Accordingly, renewed intrusive activity in central E Greenland, which lasted for more than 16 myr altogether, began in earnest broadly contemporaneous to the final stages of intrusive activity in the then neighbouring Faroe Islands. Thus, it appears reasonable to assume that the Faroese and central E Greenland regions were somewhat decoupled from one another tectonically and magmatically during the period of time that followed the onset of the main rifting event in the NE Atlantic. While regional rifting events probably governed the subsequent igneous activity in central E Greenland [25, 49], the FIBG area most likely gradually drifted away towards the ESE from axes/zones of active rifting and magmatism in the time span from ~55.5 Ma to ~50.5 Ma and later on as well, as suggested by the diminishing local igneous activity.

5.6. Faroe Islands and Seafloor-Spreading in the Early Paleogene Period

The arguments from previous sub-sections seem to suggest that the evolution of the FIBG area during relatively late stages of local Early Paleogene magmatism (i. e. from ~56.4 Ma to ~50.5 Ma), probably occurred in response to regional tectonic events related to the ultimate rifting of the NE Atlantic, which could have been somewhat different when compared to those affecting the then neighbouring regions of the north Faroe-Shetland Basin and the central E Greenland

area. With respect to earlier igneous activity in these parts of the then embryonic N Atlantic (according to previous sub-sections), it appears that central E Greenland experienced extrusive and major intrusive activity, while the Faroe Islands experienced a more quiet/hiatus period at ~57.4 Ma - ~56.3 Ma (If ± uncertainties are considered mostly theoretical.). Merely extrusive activity took place in the Faroe Islands at ~56 Ma - ~55.6 Ma (± uncertainties, Table 1.), while contemporaneous central E Greenland potentially experienced a brief hiatus period. While noticeable intrusive activity took place in the Faroe Islands at a relatively restricted period of time from ~55.5 Ma to ~50.5 Ma, intrusive activity commenced and went on for some considerable time (~53.5 Ma - ~37 Ma) in central E Greenland. These apparent differences in igneous activities seem to point to two somewhat tectonically decoupled regions, which perhaps experienced some kind of alternating magmatism during the time period from ~57.4 Ma to ~50.5 Ma? The occurrences of a number of Early/Mid Paleogene regional rifting centres, as suggested for central E Greenland earlier [25, 49] and the northern Faroe-Shetland Basin [43], would be in accordance with recent research on the NE Greenland region, where several isolated seafloor spreading events presumably triggered local magmatism and the subsequent main NE Atlantic rifting event at these latitudes [31]. Hence, if one accepts that significant proportions of neighbouring NAIP regions formed in response to regional rifting events and that the central E Greenland and Faroese regions could have been tectonically decoupled subsequent to ~57.5 Ma, it does not appear unrealistic to ascribe the bulk of the magmatic pulses, which built up the Faroe Islands in the Early Paleogene Period (From ~57.5 Ma to ~50.5 Ma ± uncertainties), to regional extension and local rifting events. In turn, these regional/local events probably developed/coalesced into a common main seafloor-spreading axis/zone themselves in the then embryonic N Atlantic.

General principles on melt production and effusion rates of e. g. basaltic lavas suggest that relatively slow effusion/intrusion rates (compound lava flows and/or smaller sills) may be associated with decompression melting at relatively slow extension/spreading rates whilst high (er) effusion/intrusion rates (laterally extensive simple/tabular lava flows and/or voluminous sills) are indicative of fast (er) extension/spreading rates [51, 52]. Accordingly, the mostly compound-type lavas of the Malinstindur Formation [13] probably point to relatively sluggish extension/spreading rates during its formation (< ~56.35 Ma). In addition to compound flows, the common occurrences of thick simple/tabular lavas in the Enni Formation (+ Sneis Fm.), indicate alternating periods with moderate versus greater rates of melting and extension/spreading towards the end of local surface magmatism in the Faroese area at around ~55.8 Ma (Table 1, Figure 4). Geochemical similarities between lavas of the Skrænterne and Rømer Fjord formations of central E Greenland with those of e g. the contemporaneous Faroese Enni Formation [16, 44, 45] could in theory well reflect similarities in extension rates within their respective mantle sources during melting, thus resulting in broadly similar igneous products.

Recent research on the north Faroe-Shetland Basin region identified an initial line of continental-breakup located ~50 km to the NNW off the Faroe Islands in the Early Paleogene Period [43]. Accordingly, the oldest Faroese sills (The low-TiO_2 Streymoy and Kvívík sills; the high-TiO_2 Eysturoy and Sundini sills) were emplaced on average ~75 km from the incipient seafloor spreading axis. If an average spreading rate of ~0.013 m per year for the last ~56 myr is accepted for the eastern fringes of the evolving N Atlantic rift system, the distances to the active rift system of the younger Faroese sills during their emplacement were: For the Svínoy-Fugloy Sill (average age ~54.4 Ma) the distance was around 89.3 km; for the Morskranes Sill (age ~53.2 Ma) the distance was approximately 104.9 km and the Vestmanna and Langaregn sills (average age ~50.5 Ma) were on average emplaced 140 km from the then active rifting axis. Consequently, the observed decrease in sill sizes/volumes with decreasing ages seem to reflect a decrease in local igneous activity with increasing distances to the active N Atlantic rift system, i. e. crustal extension rates within the actual region apparently abated gradually and finally came to a more or less standstill in the matter of ~5 to 5.3 myr following the initial breakup. In this context it is worth noticing, that an absence of mutual alignments between dykes that initially fed the Faroese sills and between dykes/chimneys emanating from a few of these seemingly point to a near-absence of extension-related stress fields in the uppermost crust during their intrusive phases. The sills themselves however, did generate compression-related stresses in their host basalts upon their vigorous intrusions and subsequent inflations/evolvements.

5.7. Potential Depths of Origin for Early Paleogene Faroese Mafic Melts

When it comes to basaltic lavas and intrusive rocks of various ages building up the various regions of the NAIP, these are customarily grouped into high-TiO_2 versus low-TiO_2 basaltic compositions. The former are commonly interpreted to have formed by low-degree melting of suitable mantle materials at noticeable depths (I. e. at relatively high pressure), while the latter are often interpreted to have formed by larger degrees of mantle melting at relatively shallower mantle depths (I. e. at relatively low pressure). Recent studies on petrogenetic evolutions of Faroese basaltic rock suites and of similar rock types the NW European margin, employed TiO_2 compositions in order to distinguish between formation of basaltic magmas at deep versus shallower mantle levels [8, 43, 45]. These authors infer a lithosphere base that was more or less smooth with relatively continuous and gradual transitions between thick and thinner lithosphere, following its extension and stretching. In reality however, the LAB, the depth of which may be important for the extent of mantle melting to produce basaltic magmas [36], could in reality vary noticeably over relatively short geographical distances in some igneous regions, depending on their previous tectonic histories [30, 42, 53]. In the context of high-TiO_2 versus low-TiO_2 compositions in basaltic magmas, it

is pertinent to note that TiO_2 contents in such magmas are not particularly sensitive to pressure during melting, but rely chiefly on the degrees of melting of suitable sources, where TiO_2 contents decrease with increasing degrees of melting irrespective of ambient pressure conditions [54, 55]. Also, TiO_2 contents in basaltic magmas remain relatively stable during moderate percentages of fractional crystallisation of e g. plagioclase and pyroxenes from these [11]. Source fertility and content of fluids in actual mantle sources, in addition to a ready supply of heat so as to increase local temperatures govern overall melting percentages (Table 2). In turn, temperatures required to reach some local solidus (TS) or temperatures in excess of the local solidus (TE) can be gained by either heat supply from lower local stratigraphic levels at fixed pressures or by local adiabatic upwelling so as to initiate and/or maintain local decompression melting [36].

Table 2. *Changes in solidus ttemperatures, melt percentages and major element compositions as functions of changes in physical conditions during formation of basaltic magmas by mantle melting.*

	[a, b]**Increasing fertility (basaltic material added?)**	[c; d; e; f]**Increasing temperature (fixed pressure)**	[a; e; f, g]**Increasing pressure (fixed temperature)**	[b; f; g, h]**Increasing % melting (fixed temp. and press.)**	[h; i]**Increasing fluid/H_2O content (Metasomatism?)**
Solidus	Decreasing P_O		Increasing P_O		Decreasing P_O
Melt %	Increasing	Increasing	Decreasing		Increasing
SiO_2		[j]Decreasing - [k]Increasing	Decreasing	[l]Decreasing - [m]Increasing	
Al_2O_3		decreasing		Decreasing	decreasing
FeO_{tot}	Increasing	Increasing	Increasing	Increasing	Increasing
MgO		Increasing		Increasing	Increasing
CaO		[j]Increasing - [k]Decreasing		[l]Increasing - [m]Decreasing	
Na_2O		Decreasing		Decreasing	
TiO_2		Decreasing	Slight increase	Decreasing	

Superscript letters from a to i point to studies of: a[56]; b[57]; c[58]; d[59]; e[60]; f[54, 55]; g[61]; h[62]; i[63]. jValid at temperatures below ~1350° C; kValid at temperatures above ~1350°C; lValid at melting percentages lower than ~15%; mValid at melting percentages larger than ~15%. PO refer to pressure (GPa) at solidus.

A relatively wide span of melting percentages of slightly heterogeneous mantle sources have the potential to produce basaltic magmas of variable TiO_2 compositions, where ~4.5% to ~7.5% and ~16% to ~21% mantle melting of variously metasomatised or enriched lherzolitic sources would result in high-TiO_2 and low-TiO_2 basaltic magmas respectively [11]. If high-TiO_2 basaltic magmas in general are derived from melting at relatively fixed high pressures and < ~5% mantle melting: [11, 20] and refs. therein, a slowly ascending vertical column of mantle sources of around 50 kilometres and covering a considerable geographical extent would be required in order to produce the ~2.5 km high-TiO_2 main/middle section of the Beinisvørð Formation, as reported previously [13]. Obviously, substantial additional mantle melting would be required in order to produce the remaining high-TiO_2 (and low-TiO_2) basaltic rocks of the FIBG.

With respect to geochemical 'evidences' on formation of basaltic melts that display 'garnet signature', most often interpreted to have formed at deep mantle levels by melting within the garnet-lherzolite stability field, recent research suggests that pooled and near-fractionated melts of compositionally and thermally variable peridotites in the spinel-lherzolite and plagioclase-lherzolite stability fields commonly display similar highly variable trace element and isotope garnet signatures [64]. Mantle sources from a number of central European localities, which underwent previous rifting/extension events, commonly contain compositionally variable sub-continental lithospheric mantle (SCLM) xenoliths that in turn are intensely metasomatised by alkali or silica-saturated/oversaturated basaltic melts, which formed by low-percentage melting within the underlying asthenospheric mantle [65, 66].

Therefore, upper parts of the asthenosphere and lower parts of the SCLM in any areas, previously exposed to extension/rifting and/or subduction-related processes, could have been pervasively laced with comparable metasomatic agents. Hence, it may be envisaged that intensely metasomatised mantle zones/regions could possess generally increased fertility, in addition to noticeable lower average/overall solidus temperatures, when compared to those of other more or less pristine mantle zones/regions. Extension across ancient suture zones, which are linked to previous constructive and/or destructive plate margins, was commonplace during formation of the NAIP and is thought to have had the potential of eroding lithospheric material from lower SCLM levels before ultimately redistributing it to the underlying asthenosphere [67]. Hence, when reflecting on the text discussed in this sub-section, it seems reasonable to expect that compositionally heterogeneous and fertile mantle zones within the NAIP existed adjacent to older suture zones, which previously experienced relatively pervasive igneous-related metasomatism and repositioning of SCLM materials. In turn, such enriched zones could have served as nucleus/seeds that triggered and generously maintained rifting and mantle melting within parts of the NAIP in the past, in preference to rifting/magmatism at/in neighbouring less affected mantle regions. Regarding the production of high-TiO_2 basaltic magmas derived from relatively deep-seated NAIP mantle sources, a scenario also involving melting at shallower mantle levels of sources comprising

metasomatised SCLM and/or asthenospheric materials, which in turn exhibit noticeably decreased solidus temperatures and markedly increased fertility, offers an appealing alternative explanation on formation of such magmas. In addition, the potential issue with garnet signatures may require more than a single explanation [64].

5.8. Early Paleogene Faroese Magmas and Lithosphere Configuration

With respect to basaltic rocks of the Faroe Islands, high-TiO_2 and low-TiO_2 lavas occur as intimately associated and alternating layers in numerous localities [8, 13, 45, 68], thus indicating a direct spatial and temporal relationship, i. e. in broad concurrence with the characteristics displayed by the four oldest Faroese sills [5, 11]. In order to properly constrain the general petrogenetic history of basaltic rocks like those of the Faroe Islands by means of their TiO_2 contents for instance, it would be advantageous to address mantle architectures as related to geography, which have the potential to noticeably influence geochemical compositions of basaltic magmas in general.

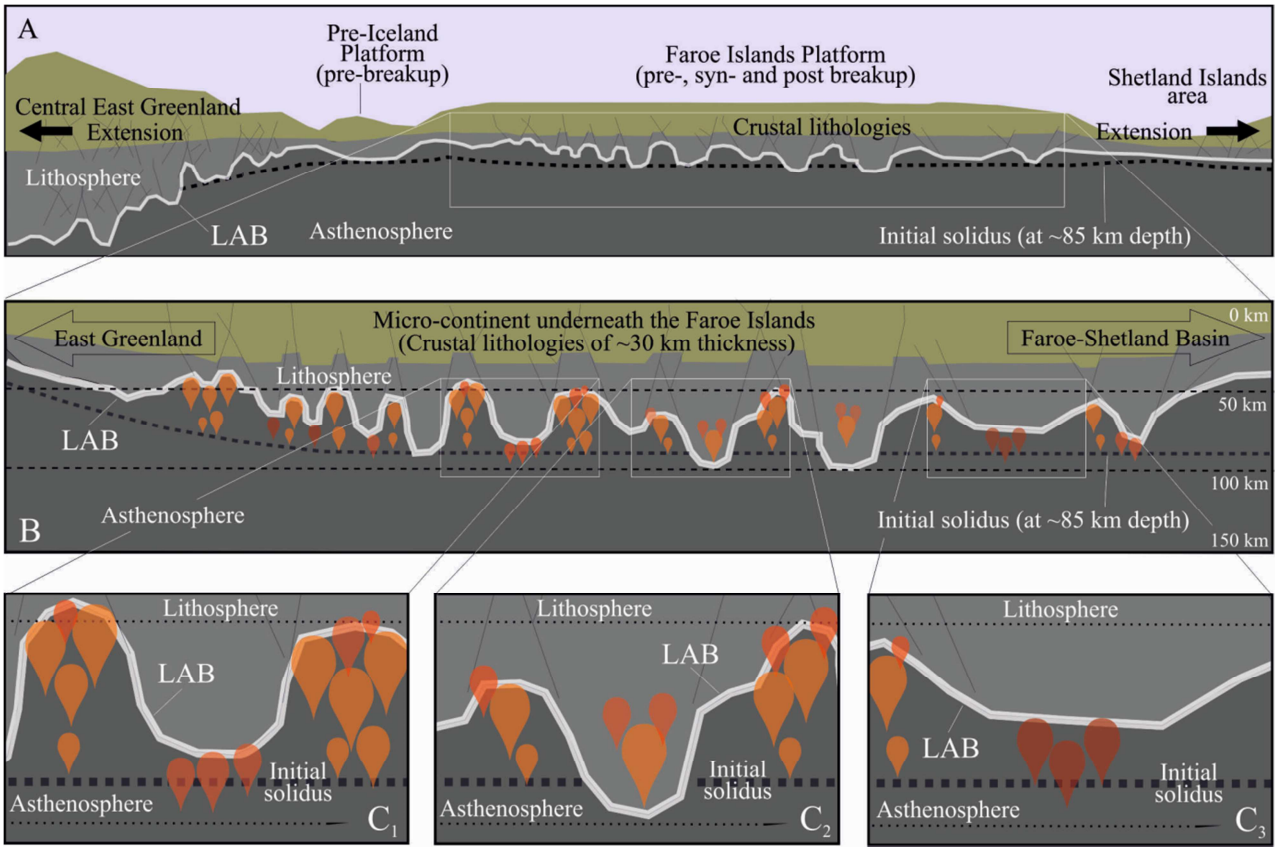

Figure 6. *Profiles indicating idealised lithosphere-asthenosphere boundaries (LAB) in the E. Greenland, Iceland, Faroe Islands and Shetland Islands regions in the Early Paleogene Period (modified general LAB geometries from an earlier study [53]. Inverted reddish droplets indicate low-percentage high-TiO_2 melts, vine-red droplets indicate moderate-percentage intermediate-TiO_2 melts, while inverted orange droplets point to relatively large-percentage low-TiO_2 melts. (A) The entire proto Faroe Islands area was affected by the extension between E Greenland and the NW European margin in the Early Paleogene Period. (B) Extension/stretching across the Faroe Islands Platform in the Early Paleogene Period triggered widespread decompression melting at mantle levels between solidus and the LAB, thus leading to the formation of high-TiO_2 and low-TiO_2 magmas. (C_1) The lid effect could have resulted in the formation of low-percentage high-TiO_2 melts at relatively deep mantle levels and higher-percentage low-TiO_2 melts at shallower mantle levels. Adiabatic ascent of noticeable quantities of low-TiO_2 magmas could have triggered low-percentage melting of particularly fertile surrounding mantle materials to produce additional low-percentage high-TiO_2 melts at relatively shallow mantle levels. In addition, one would expect a noticeable spread in TiO_2 compositions within large individual batches of magmas. Production of some high-TiO_2 melt batches from low-percentage melting of ordinary mantle lherzolites at relative shallow levels may be envisaged too, where these melts segregated from their sources prior to any low-TiO_2 melt production from larger-percentage melting. (C_2) Partly as in C., but with additional inferred melting in the sub-continental lithospheric mantle. (C_3) Partly as in C., but also with the production of intermediate-TiO_2 melts from moderate-percentage melting at moderately deep mantle levels.*

When it comes to lithosphere thicknesses and general LAB geometries in the North Atlantic area during the Early Paleogene Period, previous studies have pointed to the probable existence of ancient suture zones from previous tectonic events in literally all of the igneous regions of the NAIP, including the FIBG area [4, 5, 30, 32, 33, 67]. Consequently, it doesn't appear unreasonable to infer irregular LAB geometries, comparable to those presented by [53] for instance, for some of the igneous regions building up this LIP (Figure 6A and Figure 6B). Scenarios like those displayed in Figure 6 illustrate that mantle environments with uneven LAB geometries could have the potential to generate

melts of various geochemical compositions, during periods with crustal extension/thinning and associated adiabatic mantle upwelling. In the tentative model (s) presented in Figure 6B and Figure 6C, high-TiO_2 basaltic melts are ideally formed by low-percentage melting at relatively great mantle depths within relatively restricted vertical melting intervals, whilst their low-TiO_2 counterparts ideally formed by relatively high-percentage melting at relatively shallow mantle depths within a relatively wide vertical melting interval. We further envisage (tentatively) that high-TiO_2 basaltic magmas originating from low-percentage melting of metasomatised and/or underplated basaltic materials, occasionally formed at the peripheries of (and in response to) large volumes of hot low-TiO_2 basaltic magmas at shallow to moderate mantle depths, which pooled in the neighbourhood of the local LAB beneath the Faroese area in the Early Paleogene Period (Figure 6B and Figure 6C). In point of fact, one suitable analogue here would be the incompatible element-enriched basaltic rocks recorded for parts of the Skaergaard Intrusion, E Greenland. It formed by re-melting of some of its older parts, in the presence of trace amounts of fluids, in response to intrusive activity associated with emplacement of the adjacent basaltic Basistoppen Sill [46]. Formation of basaltic magmas from melting of fertile mantle sources and/or mantle sources variously affected by previous melting and/or metasomatising events in e. g. deep keels of the SCLM beneath the Faroese area in the Early Paleogene Period, as visualised in Figure 6B and Figure $6C_2$, remain potential options when it comes to production of both high-TiO_2 and low-TiO_2 melts at mantle depths, which did not necessarily differ noticeably from one another: previous discussion and suggestions [5, 11]. In this context it is perhaps worthwhile to reflect on the fact that all developing basaltic melts, including low-TiO_2 melts that ultimately formed by comparatively high-percentage mantle melting, went through low-percentage melting phases too during their earlier stages of formation, no matter the compositions of their mantle sources. Shouldn't it be expected that at least some of these melts ultimately segregated from their mantle sources at relatively shallow mantle levels too, when melting percentages reached 4 to 6 for instance, much as they do at deeper mantle levels?

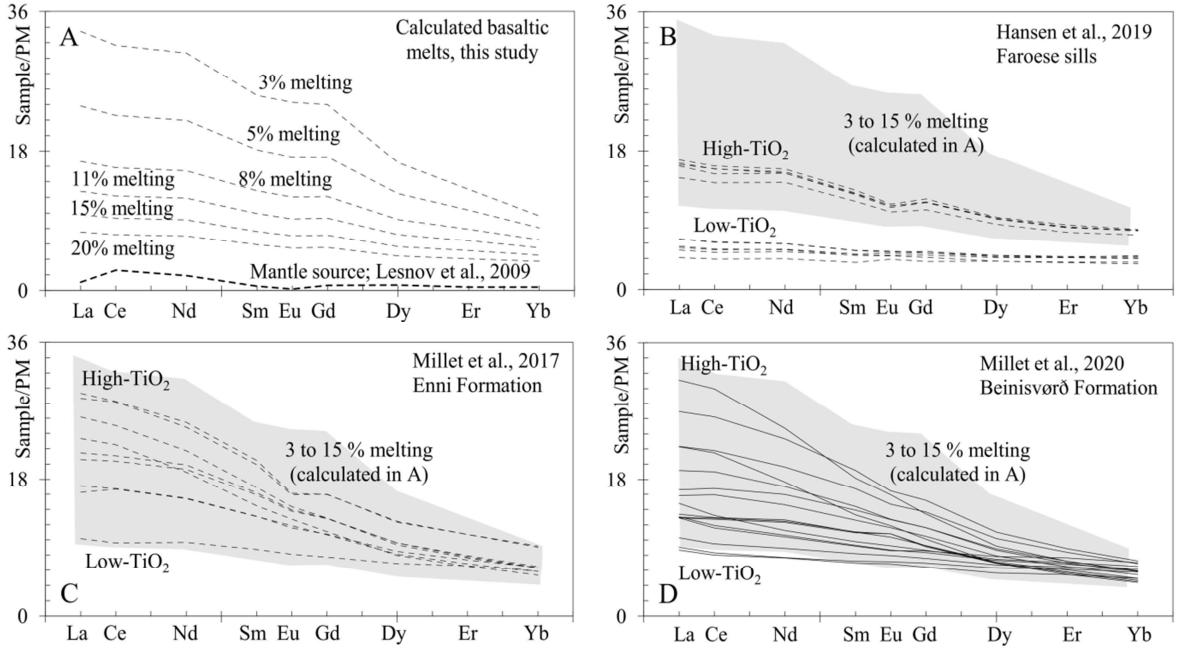

Figure 7. *REE in basaltic melts normalised to primitive mantle values (PM from McDonough and Sun [37]. (A) Batch melting calculations on REE compositions representing average values of metasomatised spinel lherzolites from Lesnov et al. [69] in the presence of residual olivine (84 %), orthopyroxene (15.5 %) and spinel (0.5 %). Mineral/melt partition coefficients and batch melting equation are from Rollinson [70] and refs. therein). The LREE tend to become relatively much more enriched than do their MREE and HREE in particular with decreasing percentages of calculated melting. (B) Calculated melts (3 – 15 %) are contrasted against Faroese sills from Hansen et al. [11]. (C) Calculated melts (3 – 15 %) are contrasted against lavas of the Enni Formation from [45]. (D) Calculated melts (3 – 15 %) are contrasted against lavas of the Beinisvørð Formation from [8].*

When it comes to the oldest contemporaneous high-TiO_2 and low-TiO_2 Faroese sill groups, their close spatial relationships and differences in geochemical compositions have previously been attributed to melting of neighbouring mantle sources variously affected by metasomatism at mantle depths that did not necessarily differ much (Figure $6C_2$)[11]. These authors effectively demonstrated that various percentages of melting of fertile metasomatised mantle materials (spinel lherzolites) may adequately explain the entire range in geochemistry displayed by the Faroese basaltic sills irrespective of their TiO_2 makeup. A few additional batch melting calculations carried out in this contribution (Figure 7A) strongly suggest that an array of melting percentages of a compositionally relatively wide variety of fertile metasomatised spinel lherzolites can reproduce the REE compositions of not only the Faroese sills

(Figure 7B), but also of local high-TiO_2 and low-TiO_2 lavas such as those representing the Beinisvørð and Enni formations (Figure 7C; Figure 7D).

The tentative hypotheses put forward here regarding the bulk of Faroese igneous products initially developed from local magma sources rather than from more distant ones, suggest that chemostratigraphically similar basaltic sequences of the FIBG and East Greenland do not necessarily originate from common mantle sources situated in between these two igneous regions, as has been tentatively suggested earlier [44, 45] and refs, therein). Indeed, the age comparisons between these two igneous regions (Previous sub-sections.) suggest some degrees of contemporary differences with respect to their regional stress regimes (Principal stress axes.) and magmatic activity. An alternative mechanism, with a potential to explain chemostratigraphical similarities between e g. the Faroese Enni formation and the Skrænterne and Rømer Fjord formations of central E Greenland, would be similar lithospheric extension rates that resulted in near-identical melting percentages within broadly similar mantle sources.

As such, the potential existence of a contemporary Iceland microcontinent between central E Greenland and the developing FIBG, as suggested previously [67], would not be at odds with measurements, observations and interpretations presented in this contribution.

6. Summary and Concluding Remarks

In this contribution we present new $^{40}Ar/^{39}Ar$ ages for most of the sills exposed on the Faroe Islands, in addition to new and recalculated $^{40}Ar/^{39}Ar$ ages for some of the Faroese basaltic lava formations. Altogether, the new radiometric ages and compiled recalculated radiometric ages presented in this study point to the formation of the entire basaltic lava successions and sills of the Faroe Islands during a time interval from ~61 Ma to ~50.5 Ma, i. e. it took at least ~10.5 myr for the initial Faroese basaltic plateau and its intrusive systems to develop. As no reliable radiometric ages are available for the Faroese Lopra Formation yet, the Faroe Islands could in theory be a few hundred thousand years older than the currently recorded maximum ages. Also, volcanism to build up the Enni Formation could be slightly younger than is presented in this paper, as we do not know its initial thickness with absolute certainty. moreover, we have generally considered ± uncertainties of calculated ages to be mostly theoretical, while in reality the ages of some of these rock suites may overlap somewhat. Based on the geochronological results obtained in this study, in addition to associated tectonic and geochemical interpretations, a few inferences regarding timing and sequences of events within the FIBG during the Early Paleogene Period are presented below:

1. Subsequent to the formation of the lowermost Lopra Formation, in response to outpourings of basaltic hyaloclastic material in a shallow-marine or in a marshy sub-aerial environment at ≥ ~61 Ma, the overlying Beinisvørð Formation developed between ~61 Ma and ~57.45 Ma (~3.55 myr in total) in response to significant outpourings of magmas hosted mostly in tabular lava flows, suggestive of noticeable rates of extension/effusion.
2. The mostly sedimentary and pyroclastic Presthagi and Hvannhagi formations, residing on top of the Beinisvørð Formation, were deposited during a largely hiatus/quiescent period with reduced volcanic activity, which lasted from ~57.5 to ~56.3 Ma (~1.2 myr combined, if ± uncertainties are considered to be mostly theoretical.).
3. The Malinstindur Formation, resting atop Presthagi and Hvannhagi formations, and the overlying Sneis and Enni formations formed in the time span from ~56.35 Ma to ~55.85 Ma, i. e. within a relatively narrow time interval of ~0.5 myr (If ± uncertainties are considered to be mostly theoretical.). Increased occurrences of thick tabular/simple lava flows in the uppermost Enni Formation relative to the underlying Malinstindur Formation could point to increased local extension/effusion rates in the latest stages of local surface magmatism.
4. Subsequent to the deposition of the (presumed) top layers of the Enni Formation at ~55.85 Ma, changes in the regional stress fields triggered the formation of relatively voluminous basaltic sill intrusions in the form of the Streymoy, Kvívík, Eysturoy and Sundini sills at ~55.5 Ma to ~55.2 Ma (average ~55.35 Ma). Successively less voluminous saucer-shaped basaltic sills were intruded into the Faroese lava pile at ~54.75 Ma to ~54.05 Ma (Svínoy-Fugloy Sill, average ~54.4 Ma); at ~53.15 Ma (Morskranes Sill) and at ~50.7 Ma to ~50.3 Ma (Langaregn and Vestmanna sills, average ~50.5 Ma). The ± age uncertainties for these are considered to be mostly theoretical too.
5. Comparison between radiometric ages measured for rock suites of the Faroe Islands and central E Greenland seem to suggest that igneous activity in (parts of) these two neighbouring NAIP regions were partly or wholly decoupled from time to time subsequent to around 57.5 Ma.

With respect to suitable mantle sources, the melting of which gave rise to the igneous products that built up the initial Faroese lava plateau in the Early Paleogene Period, a few petrogenetic models have been presented in earlier studies, most of which have the potential to explain much of measured and observed characteristics typical for the FIBG. In this contribution we point to an alternative approach regarding basaltic melt formation in a mantle environment with an irregular LAB configuration. We speculate that some of the precursor magmas building up the Faroese archipelago may have formed initially at various mantle depths by various percentages of melting of suitable mantle sources adjacent to an irregular LAB, thus providing high-TiO_2 and low-TiO_2 basaltic magmas. Other local magmas, giving rise

to some of the Faroes sills for instance, may have formed at roughly equal mantle depths by varying percentages of melting of metasomatised/fertile spinel lherzolite sources. We envisage general sub-vertical transport of the molten rocks, which initially built up Faroese lavas and sills, via multiple feeder systems, which themselves in turn were supplied from multiple magma sources generated over relatively wide geographic areas within the FIBG region.

Future Works

It would be desirable to acquire some additional $^{40}Ar/^{39}Ar$ radiometric ages representing a number of Faroese lava horizons, notably from the Beinisvørð, Malinstindur, Sneis and Enni formations within the foreseeable future, in addition to a few supplementary radiometric ages representing selected local sills (Research is in progress).

Data Availability

Diagrams depicting cumulative % ^{39}Ar released versus K/Ca ratios as well as isochron plots for relevant sill and lava samples, from Table 1 and Figure 2, are shown in electronic Supplement A, published in Mendeley Data, Hansen and Ganerød, March 2023a:

https://doi.org/10.17632/87gtjjh5gb.5

Detailed geological maps of the Faroe Islands, showing geographical sample localities, photomicrographs illustrating the petrography of relevant basaltic rock samples and, plots illustrating MgO compositions versus other major element oxides are depicted in Figure A, Figure B, Figure C and Table A in electronic supplement B, which was published in Mendeley Data, Hansen and Ganerød, March 2023b:

https://doi.org/10.17632/2y29tsw7nh.1

Author Contributions

JH was responsible for sample collection and sample preparation for quality check. JH also produced the bulk of the actual paper. MG was responsible for everything related to acquirement of radiometric data, which are shown in Table 1, Figure 2 and in diagrams displayed in electronic Supplement A, in addition to providing description of analytical techniques.

Disclaimer

The authors declare that they have no conflict of interest and nothing to disclaim.

Acknowledgments

Funding from an anonymous contributor is much appreciated. Constructive critique by an anonymous senior geologist on an earlier version of the manuscript is acknowledged. The paper benefited from constructive reviews by two anonymous reviewers.

References

[1] Saunders, A. D., Fitton, J. G., Kerr, A. C., Norry, M. J. and Kent, R. W. (1997). The North Atlantic Igneous Province: Geophys. Monogr. 100, 45-93.

[2] Saunders, A. D. (2016). Two LIPs and two Earth-system crises: the impact of the North Atlantic Igneous Province and the Siberian Traps on the Earth-surface carbon cycle: Geol. Mag. 153 (2), 201-222. doi: 10.1017/S0016756815000175.

[3] Wilkinson, C. M., Ganerød, M., Hendriks, B. W. H. and Eide, E. A. (2016). Compilation and appraisal of geochronological data from the North Atlantic Igneous Province (NAIP): Geol. Soc. London Spec. Publ. 447. http://doi.org/10.1144/SP447.10.

[4] Hansen, J., Jerram, D. A., McCaffrey, K. J. W. and Passey, S. R. (2009). The onset of the North Atlantic Igneous Province in a rifting perspective: Geol. Mag. 146 (3), 309-325. https://doi.org/10.1017/S0016756809006347.

[5] Hansen J. (2011). Petrogenetic Evolution, Geometries and Intrusive Styles of the Early Cenozoic Saucer-Shaped Sills of the Faroe Islands: Doctoral thesis, Durham University, http://etheses.dur.ac.uk/3631/.

[6] Á Horni, J. A., Hopper, J. R., Blischke, A., Geisler, W. H., Stewart, M., McDermott, K. H., Judge, M., Erlendsson, Ö. and Árting, U. E. (2017) Regional distribution of volcanism within the North Atlantic Igneous Province: Geol. Soc. London, Spec. Publ. 447, 105-125. http://doi.org/10.1144/SP447.18.

[7] Meyer, R., Van Wijk, J. and Gernigon, L. (2007). The North Atlantic Igneous Province: A review of models for its formation: Geol. Soc. Am. Spec. Pap. 430, 525-52.

[8] Millet, J. M., Hole, M. J., Jolley, D. W., Passey, S. R. and Rosetti, L. (2020). Transient mantle cooling linked to regional volcanic shut-down and early rifting in the North Atlantic Igneous Province: Bull. Volcan. 82: 61, 27. https://doi.org/10.1007/s00445-020-01401-8.

[9] Storey, M., Duncan, R. A. and Tegner, C. (2007). Timing and duration of volcanism in the North Atlantic Igneous Province: implications for geodynamics and links to the Iceland hotspot: Chem. Geol. 241, 264-281. doi: 10.1016/j.chemgeo.2007.01.016.

[10] Hansen, J., Jerram, D. A., McCaffrey, K. J. W. and Passey, S. R. (2011). Early Cenozoic saucer-shaped sills of the Faroe Islands: an example of intrusive styles in basaltic lava piles, J. Geol. Soc. London 168 (1), 159-178.

[11] Hansen, J., Davidson, J. P., Jerram, D. A., Ottley, C. J. and Widdowson, M. (2019). Contrasting TiO_2 compositions in Early Cenozoic mafic sills of the Faroe Islands: an example of basalt formation from distinct melting regimes: Earth Sci. 8 (5), 235-267. http://www.sciencepublishinggroup.com/j/earth doi: 10.11648/j.earth.20190805.11.

[12] Hansen, J. (2020). Transgressive sills and lateral lava flows: on the visual observation of igneous sheets in rugged mountainous terrains and the optical illusion factor: Earth Sci. 9 (5), 164-177. doi: 10.11648/j.earth.20200905.13.

[13] Passey, S. R. and Jolley, D. W. (2009). A revised lithostratigraphic nomenclature for the Palaeogene Faroe Islands Basalt group, NE Atlantic Ocean: Earth Environm. Sci. Trans. Royal Soc. Edinb. 99 (3-4), 127-158. https://doi.org/10.1017/S1755691009008044.

[14] Hansen J. (2015). A numerical approach to sill emplacement in isotropic media: Do saucer-shaped sills represent 'natural' intrusive tendencies in the shallow crust?: Tectonophys. 664, 125–138. http://dx.doi.org/10.1016/j.tecto.2015.09.006.

[15] Tarling, D. H. and Gale, N. H. (1968). Isotopic dating and palaeomagnetic polarity in the Faeroe Islands: Nature, 218, 1043-1044.

[16] Waagstein, R. (1988). Structure, composition and age of the Faeroe basalt plateau: Geol. Soc. London Spec. Publ. 39, 225-238. https://doi.org/10.1144/GSL.SP.1988.039.01.21.

[17] Abrahamsen, N. (2006). Palaeomagnetic results from the Lopra-1/1A re-entry well, Faroe Islands: Geol. Surv. Denm. and Greenl. Bull. 9, 51-65.

[18] Waagstein, R., Guise, P. and Rex, D. (2002). K/Ar and $^{40}Ar/^{39}Ar$ whole-rock dating of zeolite facies metamorphosed flood basalts: the upper Paleocene basalts of the Faroe Islands, NE Atlantic: Geol. Soc. London Spec. Publ. 197, 219-252. https://doi.org/10.1144/GSL.SP.2002.197.01.09.

[19] Hansen, J. and Ganerød, M. (2023b). Sampling and evaluation of basaltic rocks of the Faroe Islands: Details on material used in geochronological $^{40}Ar/^{39}Ar$ dating of local rocks", Mendeley Data, V1, https://data.mendeley.com/datasets/2y29tsw7nh/1

[20] Holm, P. M., Hald, N. and Waagstein, R. (2001). Geochemical and Pb-Sr-Nd isotopic evidence for separate hot depleted and Iceland plume mantle sources for the Paleogene basalts of the Faroe Islands: Chem. Geol. 178, 95-125. https://doi.org/10.1016/S0009-2541(01)00260-1.

[21] McDougall, I. and Harrison, T. M. (1999). Geochronology and Thermochronology by the $^{40}Ar/^{39}Ar$ Method: Oxford University Press, pp. 269.

[22] Renne, P. R., Mundil, R., Balco, G., Min, K. and Ludwig, K. R. (2010). Joint determination of ^{40}K decay constants and $^{40}Ar*/^{40}K$ for the Fish Canyon sanidine standard, and improved accuracy for $^{40}Ar/^{39}Ar$ geochronology: Geochim. Cosmochim. Acta, 74 (18), 5349-5367. https://doi.org/10.1016/j.gca.2010.06.017.

[23] Lee, J-Y,. Marti, K., Severinghaus, J. P, Kawamura, K., Yoo, H-S., Lee, J. B. and Kim, J. S. (2006). A redetermination of the isotopic abundances of atmospheric Ar: Geochim. Cosmochim, Acta, 70, 4507-4512. doi: 10.1016/j.gca.2006.06.1563.

[24] Hansen, J. and Ganerød, M. (2023a). Geochronology of the Faroe Islands: A case study on $^{40}Ar/^{39}Ar$ dating of local basaltic sills and selected lavas: Mendeley Data, V5, https://data.mendeley.com/datasets/87gtjjh5gb/5

[25] Tegner, C., Brooks, C. K., Duncan, R. A., Heister, L. E. and Bernstein, S. (2008). $^{40}Ar/^{39}Ar$ ages of intrusions in East Greenland: Rift-to-drift transition over the Iceland hotspot: Lithos, 101, 480-500. https://doi.org/10.1016/j.lithos.2007.09.001.

[26] Ganerød, M., Smethurst, M. A., Torsvik, T. H., Prestvik, T., Rousse, S., McKenna, C., Van Hinsbergen, D. J. J. and Hendriks, B. W. H. (2010). The North Atlantic Igneous Province reconstructed and its relation to the Plume Generation Zone: the Antrim Lava Group revisited: *Geophys. J. Internat.* 182 (1), 183-202. http://doi.org/10.1111/j.1365-246X.2010.04620.x.

[27] Svensen, H., Planke, S. and Corfu, F. (2010). Zircon dating ties the NE Atlantic sill emplacement to initial Eocene global warming: J. Geol. Soc. London, 167, 433-436. doi.1144/0016-76492009-125.

[28] Brooks, C. K. (2011). The East Greenland rifted volcanic margin: Geol. Surv, Greenl. Denm. Bull. 24, pp 97.

[29] Larsen, L. M., Pedersen, A. K., Tegner, C., Duncan, R. A., Hald, N. and Larsen, J. G. (2016). Age of Tertiary volcanic rocks On the West Greenland Continental Margin: volcanic evolution and event correlation to other parts of the North Atlantic Igneous Province: Geol. Mag. 153, 487-511. doi.10.1017/S0016756815000515.

[30] Peace, A. L., Foulger, G. R., Schiffer, C. and McCaffrey, K. J. W. (2017). Evolution of Labrador Sea–Baffin Bay: Plate or Plume Processes?: Geosci. Can. 44, 91-102. https://doi.org/10.12789/geocanj.2017.44.120.

[31] Franke, D., Klitzke, P., Barckhausen, U., Berglar, K., Berndt, C., Damm, V., Dannowski, A., Ehrhart, A., Engels, M., Funck, T., Geissler, W., Schnabel, M., Thorwart, M. and Trinhammer. P. (2019). Polyphase magmatism during the formation of the northern East Greenland continental margin: Tectonics, 38 (4), 2961-3982. doi.10.1029/2019TC005552.

[32] Gernigon, L., Franke, D., Geoffroy, L., Schiffer, C., Foulger, G. R. and Stoker, M. (2020). Crustal fragmentation, magmatism, and the diachronous opening of the Norwegian-Greenland Sea: Earth-Sci. Rev. 206 (102839), 1-37. https://doi.org/10.1016/j.earscirev.2019.04.011.

[33] Schiffer, C., Doré, A. G., Foulger, G. R., Franke, D., Geoffroy, L., Gernigon, L., Holdsworth, B., Kuznir, N., Lundin, E., McCaffrey, K. J. W., Peace, A. L., Petersen, D., Phillips, T. B., Dtephenson, R., Stoker, M. and Welford, J. K. (2020). Structural inheritance in the North Atlantic: Earth-Sci. Rev. 206 (102975). https://doi.org/10.1016/j.earscirev.2019.102975.

[34] Archer, S. G., Bergman, S. C., Iliffe, J., Murphy, C. M. and Thornton, M. (2005). Palaeogene igneous rocks reveal new insights into the geodynamic evolution and petroleum potential of the Rockall Trough, NE Atlantic Margin: Basin Res. 17, 171-201. doi: 10.1111/j.1365.2117.2005.00260.x.

[35] Niu, Y. (2020). On the cause of continental breakup: A simple analysis on driving mechanisms of plate tectonics and mantle plumes: J. As. Earth Sci. 194, 104367. http://doi.org/10.1016/j.jseaes.2020.104367.

[36] Niu, Y. (2021). Lithosphere thickness controls the extent of mantle melting, depth of melt extraction and basalt compositions in all tectonic settings on Earth – A review and new perspectives: Earth-Sci. Rev. 217 (103614), 25. https://doi.org/10.1016/j.earscirev.2021.103614.

[37] McDonough, W. F. and Sun, S.-s., 1995, The composition of the Earth: Chem. Geol. 120, 223-253.

[38] Renne, P. R., Swisher, C. C., Deino, A. L., Karner, D. B., Owens, T. L. and DePaolo, D. J. (1998). Intercalibration of standards, absolute ages and uncertainties in 40Ar/39Ar dating: Chem. Geol. 145, 117-152.

[39] Kuiper, K. F., Deino, A., Hilgen, F. J., Krijgsman, W., Renne, P. R. and Wijbrans, J. R. (2008). Synchronizing rock clocks of Earth history: Science 320 (5875), 500-504. https://doi.org/10.1126/science.1154339.

[40] Min, K., Mundil, R., Renne, P. R., and Ludwig, K. R. (2000). A test for systematic errors in $^{40}Ar/^{39}Ar$ geochronology through comparison with U/Pb analysis of a 1.1-Ga rhyolite: Geochim. Cosmochim. Acta, 64 (1), 73-98. https://doi.org/10.1016/S0016-7037(99)00204-5.

[41] Richardson, K. R., Smallwood, J. R., White, R. S., Snyder, D. B. and Maguire, P. K. H. (1998). Crustal structure beneath the Faroe Islands and the Faroe-Iceland Ridge: Tectonophys, 300, 159-180. https://doi.org/10.1016/S0040-1951(98)00239-X.

[42] Darbyshire, F. A., Dahl-Jensen, T., Larsen, T. B., Voss, P. H. and Joyal, G. (2018). Crust and uppermost-mantle structure of Greenland and the Northwest Atlantic from Rayleigh wave group velocity tomography: Geophys. J. Internat. 212, 1546-1569. doi: 10.1093/gji/ggx479.

[43] Walker, F., Schofield, N., Millet, J., Jolley, D., Hole, M. and Stewart, M. (2020). Paleogene volcanic rocks in the northern Faroe–Shetland Basin and Møre Marginal High: understanding lava field stratigraphy: Geol. Soc. London Spec. Publ. 495. https://doi.org/10.1144/SP495-2019-13.

[44] Søager, N. and Holm, P. M. (2009). Extended correlation of the Paleogene Faroe Islands and East Greenland plateau basalts: Lithos, 107, 205-215. https://doi.org/10.1016/j.lithos.2008.10.002.

[45] Millett, J. M., Hole, M. J., Jolley, D. W. and Passey, S. R. (2017). Geochemical stratigraphy and correlation within Large Igneous Provinces: The final preserved stages of the Faroe Islands Basalt Group: Lithos, 286-287, 1-15. https://doi.org/10.1016/j.lithos.2017.05.011.

[46] Wotzlaw, J-F., Bindeman, I. N., Schaltegger, U., Brooks, C. K. and Naslund, H. R. (2012). High-resolution insights into episodes of crystallization, hydrothermal alteration and remelting in the Skaergaard intrusive complex: Earth Plan. Sci. Lett. 255-256, 199-212. DOI: 10.1016/J.EPSL.2012.08.043.

[47] Naumenko-Dèzes, M. O., Nägler, T. F., Mezger, K. and Villa, M. (2018). Constraining the 40K decay constant with ^{87}Rb-^{87}Sr – ^{40}K-^{40}Ca chronometer intercomparison: Geochim. Cosmochim. Acta, 220, 235-247. https://doi.org/10.1016/j.gca.2017.09.041

[48] Harrison, J. C., Mayr, U., McNeil, D. H., Sweet, A. R., McIntyre, D. J., Eberle, J. J., Harington, C. R., Chalmers, J. A., Dam, G. and Nøhr-Hansen, H. (1999). Correlation of Cenozoic sequences of the Canadian Arctic region and Greenland; implications for the tectonic history of northern North America: Bull. Can. Petrol. Geol. 47 (3), 223-254.

[49] Larsen, L. M., Pedersen, A. K., Sørensen, E. V., Watt, W. S. and Duncan, R. A. (2013). Stratigraphy and age of the Eocene Igtertivâ Formation basalts, alkaline pebbles and sediments of the Kap Dalton Group in the graben at Kap Dalton, East Greenland: ©2013 by: Bull. Geol. Soc. Denm. 61, 1–18. ISSN 2245-7070. Baker, M. B. and Stolper, E. M. (1994). Determining the composition of high-pressure mantle melts using diamond aggregates: Geochim. Cocmochim. Acta, 58 (13), 2811-2827.

[50] Thórarinsson, S. B., Holm, P. M., Tappe, S., Heaman, L. M. and Prægel, N-O. (2016). U–Pb geochronology of the Eocene Kærven intrusive complex, East Greenland: constraints on the Iceland hotspot track during the rift-to-drift transition: Geol. Mag. 153 (1), 128-142. DOI: https://doi.org/10.1017/S0016756815000448.

[51] Walker, G. P. L. (1971). Compound and simple lava flows and flood basalts: Bull. Volcanol. 35, 579-590. https://doi.org/10.1007/BF02596829.

[52] Harris, A. J. L. and Rowland, S. K. (2009) Effusion rate controls on lava flow length and the role of heat loss: A review. From: THORDARSON, T., SELF, S., LARSEN, G., ROWLAND, S. K. & HOSKULDSSON, A. (eds) Studies in Volcanology: The Legacy of George Walker: Special Publications of IAVCEI, 2, 33– 51. Geol. Soc. London, 1750-8207. https://doi.org/10.1144/IAVCEl002.3.

[53] Rychert, C. A., Harmon, N., Constable, S. and Wang, S. (2020). The Nature of the Lithosphere - Asthenosphere Boundary: Journ. Geophys. Res. Solid Earth, 125, e2018JB016462, 39. DOI: 10.1029/2018jb016463.

[54] Kinzler, R. J. (1997). Melting of mantle peridotite at pressures approaching the spinel to garnet transition: Application to mid-ocean ridge basalt petrogenesis: J. Geophys. Res. 102 (B1), 853-874. https://doi.org/10.1029/96JB00988.

[55] Collinet, M., Medard, E., Charlier, B., Auwera, J. V. and Grove, T. L. (2015). Melting of the primitive martian mantle at 0.5–2.2 GPa and the origin of basalts and alkaline rocks on Mars: Earth Sci. Plan. Lett. 427, 83-94. https://doi.org/10.1016/j.epsl.2015.06.056.

[56] Yaxley, G. M. (2000). Experimental study of the phase and melting relations of homogeneous basalt + peridotite mixtures and implications for the petrogenesis of flood basalts: Contrib. Mineral. Petrol. 139, 326-338.

[57] Kogiso, T., Hirose, K. and Takahashi, E. (1998). Melting experiments on homogeneous mixtures of peridotite and basalt: application to the genesis of ocean island basalts: Earth Plan. Sci. Lett. 162, 45-61.

[58] Baker, M. B. and Stolper, E. M. (1994). determining the composition of high-pressure mantle melts using diamond aggregates. Geochim. Cocmochim. Acta, 58 (13), 2811-2827.

[59] Ulmer, P. (2001). Partial melting inj the mantle wedge the role of H_2O in the genesis of mantle-derived 'arc-related' magmas: Phys. Earth Plan. Int. 127, 215-232. https://doi.org/10.1016/S0031-9201(01)00229-1.

[60] Falloon, T. J., Green, D. H., Danyushevsky, L. V. and McNeill, A. W. (2008). The composition of near-solidus partial melts of fertile peridotite at 1 and 1.5 GPa: implications for the petrogenesis of MORB: J. Petrol. 49 (4), 591-613.

[61] Hirose, K. and Kushiro, I. (1993). Partial melting of dry peridotites at high pressures: Determination of compositions of melts segregated from peridotite using aggregates of diamond: Earth Plan. Sci. Lett. 114, 477-489.

[62] Hirose, K. and Kawamoto, T. (1995). Hydrous partial melting of lherzolite at 1 GPa: The effect of H_2O on the genesis of basaltic magmas: Earth Plan. Sci. Lett. 133, 463-473.

[63] Green, D. H. and Falloon, T. J. (2005). Primary magmas at mid-ocean ridges, "hotspots," and other intraplate settings: Constraints on mantle potential temperature. in Foulger GR, Natland JH, Presnall DC, Anderson DL, eds., Plates, plumes, and paradigms: Geol. Soc. Am. Spec. Pap. 388, 217-247. https://doi.org/10.1130/0-8137-2388-4.217.

[64] Krein, S. B., Behn, M. D. and Grove, T. L. (2020). Origins of major element, trace element and isotope garnet signatures in mid-ocean ridge basalts: J. Geophys. Res. Solid Earth, 125 (12), pp. 33. https://doi.org/10.1029/2020JB019612.

[65] Patkó, L., Liptai, N., Aradi, L. E., Klébesz, R., Sendula, E., Bodnar, R. J., Kovács, I. J., Hidas, K., Cesare, B., Novák, A., Trásy, B. and Szabó, C. (2020). Metasomatism-induced wehrlite formation in the upper mantlebeneath the Nógrád-Gömör Volcanic Field (Northern Pannonian Basin): Evidence from xenoliths: Geosci. Front. 11 (3), 943-964. https://doi.org/10.1016/j.gsf.2019.09.012.

[66] Puziewicz, J., Matusiak-Malek, M., Ntaflos, T., Grégoire, M., Kaszmarek, M-A., Aulbach, S., Ziobro, M. and Kukula, A. (2020). Three major types of subcontinental lithospheric mantle beneath the Variscan Orogen in Europe: Lithos, 362-363, 105467. https://doi.org/10.1016/j.lithos.2020.105467.

[67] Foulger, G. R., Doré, T., Emeleus, C. H., Franke, D., Geoffroy, L., Gernigon, L., Hey, R., Holdsworth, R. E., Hole, M., Höskuldsson, Á., Julian, B., Kusznir, N., Martinez, F., McCaffrey, K. J. W., Natland, J. H., Peace, A. L., Petersen, K,. Stephenson, R. and Stoker, M. (2020). The Iceland Microcontinent and a continental Greenland-Iceland-Faroe Ridge: Earth-Sci. Rev. 206, 102926. https://doi.org/10.1016/j.earscirev.2019.102926.

[68] Søager, N. and Holm, P. M. (2011). Changing compositions of the Iceland plume; Isotopic and elemental constraints from the Paleogene Faroe flood basalts: Chem. Geol. 280, 297-313. https://doi.org/10.1016/j.chemgeo.2010.11.017.

[69] Lesnov, F. P., Koz'menko, O. A., Nikolaeva, I. V. and Palesskii, S. V. (2009). Residence of incompatible trace elements in a large spinel lherzolite xenolith from alkali basalt of Shavaryn Tsaram-1 paleovolcano (western Mongolia), Russ. Geol. Geophys. 50 (12), 1063-1072. https://doi.org/10.1016/j.rgg.2009.11.005.

[70] Rollinson, H. (1993). Using geochemical data: evaluation, presentation, interpretation, Longman, 352. https://doi.org/10.4324/9781315845548.